Doctoral Dissertation (Shinshu University)

Study on Measurement of Water Transport in Fabrics

March 2014

Chunhong ZHU

Table of Contents

Table of Contents i

List of Figures iv

List of Tables ix

Chapter 1 Introduction 1

1.1 Liquid transport in textile 2

1.1.1 Wetting of fibrous assembly 2

1.1.2 Wicking 4

1.2 Wicking processes and mechanisms 7

1.2.1 Wicking processes 7

1.2.2 Wicking mechanisms 8

1.3 Previous study on the liquid transport within fabrics 10

1.4 The purpose of this study 13

1.5 Composition of this study 14

Chapter 2 Wicking theory and measurement method 22

2.1 Wicking theory 22

2.2 Measurement method used in this study 26

2.2.1 Measurement theory 26

2.2.2 Temperature sensor used in this study 27

2.2.3 Verification of commercial thermocouples 31

Chapter 3 Change of temperature of cotton and polyester fabrics during wetting and drying 37

3.1 Introduction 37

3.2 Experimental 40
3.2.1 Manufacture of thermocouple-equipped fabric 40
3.2.2 Temperature distribution measurements 42
3.3 Results and discussions 46
3.3.1 Feasibility of thermocouples on fabric 46
3.3.2 Temperature changes in wetted fabrics 47
3.4 Development of thermocouple-equipped woven fabric 58
3.5 Conclusion 61
Chapter 4 A new thermocouple technique for the precise measurement of in-plane capillary water flow within fabrics 66
4.1 Introduction 66
4.2 Basic theory for the in-plane capillary liquid flow 69
4.3 Experimental 70
4.3.1 Experimental for measuring capillary liquid flow 70
4.3.2 Predicting water content based on temperature differences in fabrics 75
4.4 Results and discussion 78
4.4.1 The feasibility of the thermocouple method 78
4.4.2 Predicting water content from equilibrium temperature of fabric 87
4.5 Conclusion 91
Chapter 5 Effect of fabric structure and yarn on capillary liquid flow within fabrics ... 95
5.1 Introduction 95
5.2 Basic theory 98
5.3 Experimental 99
5.3.1 Test apparatus 99

5.3.2 Test samples 99
5.4 Results and discussion 103
5.4.1 Effect of weave density on the wicking coefficient of fabric 103
5.4.2 Effect of weft yarn on the wicking coefficient of fabric 107
5.5 Conclusion 112
Chapter 6 Conclusion 117
Published papers 120
Acknowledgments 121

List of Figures

Figure 1.1 Equilibrium state of a liquid drop on a solid surface: (a) contact angle between 0 and 90 °; (b) contact angle between 90 °and 180 °. 4

Figure 1.2 Wetting phenomena: (a) immersion; (b) capillary sorption; (c) adhesion; (d) spreading. 4

Figure 1.3 Wicking in a capillary system. 6

Figure 2.1 Capillary action. 23

Figure 2.2 The Seebeck effect. 28

Figure 2.3 Structure of T-type thermocouple..... 29

Figure 2.4 The image of weld machine: (a) the weld machine (A. power; B. volume; C. holder; D. operating button); (b) the detail of Part C..... 30

Figure 2. 5 Temperature measurement devices relayed to a computer. 30

Figure 2. 6 Interface of temperature recording and saving software. 31

Figure 2.7 Temperature comparison measured by precision and commercial thermometer. 33

Figure 2.8 Temperature measured by T-type thermocouples and F100 Precision Handheld Thermometer. 34

Figure 3.1 Basic structure of fabric thermocouple. 41

Figure 3.2 Image of an actual fabric thermocouple: (a) the actual thermocouple-equipped polyester fabric; (b) detail of the temperature sensor. 41

Figure 3.3 Multipoint thermocouple-equipped fabric. 42

Figure 3.4 Schematic of temperature measurement instrumentation. 43

Figure 3.5 Diagram of the spot test. 43

Figure 3.6 Ambient temperature measurements by cotton. 47
Figure 3.7 Ambient temperature measurements by polyester. 47
Figure 3.8 Temperature of wetted cotton fabric at 65% RH. 49
Figure 3.9 Temperature of wetted polyester fabric at 65% RH. 49
Figure 3.10 Temperature changes on the dropped point. 50
Figure 3.11 Mass loss during drying process at 65%RH. 53
Figure 3.12 Temperature and mass change of the two fabrics. 55
Figure 3.13 Temperature change with time of point 1. 56
Figure 3.14 Temperature change with time of point 2. 56
Figure 3.15 Initial temperature increases at point 2 on cotton fabric. 57
Figure 3.16 Structure of textile thermocouple fabric. 58
Figure 3.17 Three parts of fabric. 59
Figure 3.18 Weft cross section of fabric. 59
Figure 3.19 Real object of the thermocouple-equipped woven fabric. 60
Figure 4.1 Capillary action for in-plane capillary liquid flow. 69
Figure 4.2 Thermocouple test apparatus: (a) Schematic diagram of thermocouple method; (b) Block diagram of the overall system. 71
Figure 4.3 Temperature variations over time in a cotton/polyester fabric. 73
Figure 4.4 Diagram of a typical fabric sample as used in water flow trials. 75
Figure 4.5 A typical fabric strip sample as used in equilibrium water flow trials, showing thermocouple locations. 77
Figure 4.6 Comparison of the results of thermocouple and Byreck measurements for cotton fabric in the warp direction: (a) Relationship between the wicking length and time; (b) Relationship between wicking length and square root of time. . 80

Figure 4.7 Comparison of the results of the two measurements for cotton fabric in the weft direction: (a) Relationship between the wicking length and time; (b) Relationship between wicking length and square root of time..... 80
Figure 4.8 Comparison of the results of the two measurements for cotton fabric in the 45º bias direction: (a) Relationship between the wicking length and time; (b) Relationship between wicking length and square root of time..... 81
Figure 4.9 Comparison of the results of the two measurements for cotton/polyester fabric (C/P-1) in the warp direction: (a) Relationship between the wicking length and time; (b) Relationship between wicking length and square root of time. 81
Figure 4.10 Comparison of the results of the two measurements for cotton/polyester fabric (C/P-1) in the weft direction: (a) Relationship between the wicking length and time; (b) Relationship between wicking length and square root of time.. 82
Figure 4.11 Comparison of the results of the two measurements for cotton/polyester fabric (C/P-1) in the bias direction: (a) Relationship between the wicking length and time; (b) Relationship between wicking length and square root of time.. 82
Figure 4.12 Comparison of the results of the two measurements for cotton/polyester fabric (C/P-2) in the warp direction: (a) Relationship between the wicking length and time; (b) Relationship between wicking length and square root of time. 83
Figure 4.13 Comparison of the results of the two measurements for cotton/polyester fabric (C/P-2) in the weft direction: (a) Relationship between the wicking length and time; (b) Relationship between wicking length and square root of time.. 83
Figure 4.14 Comparison of the results of the two measurements for cotton/polyester

fabric (C/P-2) in the bias direction: (a) Relationship between the wicking length and time; (b) Relationship between wicking length and square root of time.. 84
Figure 4.15 Comparison of the results of the two measurements for cotton knit fabric (C-k) in the warp direction: (a) Relationship between the wicking length and time; (b) Relationship between wicking length and square root of time..... 84
Figure 4.16 Comparison of the results of the two measurements for cotton knit fabric (C-k) in the weft direction: (a) Relationship between the wicking length and time; (b) Relationship between wicking length and square root of time..... 85
Figure 4.17 Comparison of the results of the two measurements for cotton knit fabric (C-k) in the bias direction: (a) Relationship between the wicking length and time; (b) Relationship between wicking length and square root of time..... 85
Figure 4.18 Comparison of wicking coefficient results of different fabric samples in three directions from the thermocouple and Byreck method. 87
Figure 4.19 Relationship between water content and fabric temperature during the drying process of all fabric samples. 88
Figure 4.20 Comparison of results obtained by weighing method and thermocouple array method. 90
Figure 5.1 Schematic of modified thermocouple method. 99
Figure 5.2 Yarn specimen for experimental trial. 102
Figure 5.3 Wicking coefficient against weft weave density for cotton fabric. 104
Figure 5.4 The relationship between crimp and wicking coefficient of weft yarn. 106
Figure 5.5 Relationship between porosity and wicking coefficient for a range of cotton fabrics. 107
Figure 5.6 Wicking coefficients of different fabrics versus wicking coefficients of

weft yarns. 109

Figure 5.7 SEM images of cross sections for four yarns: (a) cotton yarn; (b) polyester yarn; (c) weft yarn for C/P-1 fabric; (d) weft yarn for C/P-2 fabric.....110

Figure 5.8 SEM images of longitudinal sections for four yarns: (a) cotton yarn; (b) polyester yarn; (c) weft yarn for C/P-1 fabric; (d) weft yarn for C/P-2 fabric. 111

List of Tables

Table 3.1 Specification of fabrics 40

Table 3.2 Testing conditions of thermocouple-equipped fabric. 44

Table 3.3 The relative humidity of micro-climate at the dropped point 52

Table 4.1 Specifications of test samples. 74

Table 4.2 Wicking coefficients ($cm/s^{0.5}$) obtained for fabric samples in three directions with two methods 86

Table 5.1 Weaving parameters of fabric samples. 100

Table 5.2 Physical properties of fabric samples. 101

Table 5.3 Gain in wicking coefficients of fabrics for warp and weft yarns and fabrics. 105

Chapter 1
Introduction

Chapter 1 Introduction

There are two aspects of wear comfort for clothing [1]. The first one is the thermo-physiological wear comfort which concerns the heat and moisture transport properties of clothing and the way that clothing helps to maintain the heat balance of the body during various levels of activity. The second one is the skin sensational wear comfort which concerns the mechanical contact of the fabric with the skin, its softness and pliability in movement and its lack of prickle, irritation and cling when damp. The heat and moisture transfer properties of fabrics are especially significant, as they play a vital role in determining the thermal comfort associated with wearing the materials. The thermal comfort of the wearer is of course greatly dependent on their clothing, in conjunction with their level of physical activity and environmental factors, since a garment may or may not be conductive to the passage of heat and moisture through its structure [2].

Moisture is transmitted through fabrics in two ways [1]:

(1) By diffusion of water vapor through the fabric. This appears to be independent of fiber type but is governed by the fabric structure. The measurement of air flow through the fabric provides a good guide to its ability to pass water vapor in large quantities.

(2) By the wicking of liquid water away from the skin using the mechanism of capillary transport. The ability of a fabric to do this is dependent on the surface properties of the constituent fibers and their total surface area.

1.1 Liquid transport in textile

Liquid transport is an important phenomenon in the processing and applications of fibrous materials. Some attentions have been paid on various aspects of liquid-fiber interactions both in terms of fundamental research and for product and process development, such as wetting, transport, and retention[3]. Moreover, liquid transport within fabrics is important in the comfort of clothing. All clothing involves the interaction of liquid or vapor with textile materials. During wearing, a person gives off perspiration which is removed from the skin through clothing [4]. The transport of liquid in textiles involves two processes: wetting and wicking. Wetting is the displacement of a solid-air (vapor) interface with a solid-liquid interface. Spontaneous transport of liquid driven into a porous system by capillary forces is termed “wicking”. As capillary forces are caused by wetting, wicking is a result of spontaneous wetting [5]. Wetting is a prerequisite for wicking. A liquid that does not wet fibers of course cannot wick into a fabric. The wetting and wicking behavior of the fibrous structure is an important aspect of performance of products, such as sportswear, hygiene disposable materials, and so on.

1.1.1 Wetting of fibrous assembly

Wetting of a fibrous assembly affects many manufacturing processes and the end use performance of materials. In a broader sense, “wetting” is used to describe the replacement of a solid-liquid or liquid-air interface with a liquid-liquid interface and a solid-air interface with a solid-solid interface. Wetting is a dynamic process [5].

For a liquid to move in a fibrous medium, it must wet the fiber surfaces before being transported through the interfiber pores by means of capillary action [6].

According to Harnett and Mehta [7], wettability describes the initial behavior of a fabric, yarn or fiber when brought into contact with liquid, for example, prior to any wicking taking place. For a liquid to wet the solid completely, the solid surface should have sufficient surface energy to overcome the free surface energy of the liquid, which refers to the surface tension, and is quantified as force per length. Fabric wettability is determined by the chemical nature of constituent fibers surface and the fiber geometry [8].

Figure 1.1 shows the three-phase thermodynamic equilibrium condition that exists for a drop of liquid resting at equilibrium on a solid surface. The forces involved in this equilibrium are given by the Young-Dupre equation [9, 10]:

$$\gamma_{SV} - \gamma_{SL} = \gamma_{LV} \cos\theta, \tag{1.1}$$

where γ is the interfacial tension that exists between the various combinations of solid, liquid and vapor. The subscripts *S*, *V*, *L* represents solid, vapor and liquid, and θ is the contact angle, shown in Figure 1.1. Contact angle is determined by three interfacial tensions (γ_{SV}, γ_{SL} and γ_{LV}). If the surface tension between the solid-vapor (γ_{SV}) is higher than the surface tension between the solid-liquid (γ_{SL}), the driving force moves towards a low tension producing spontaneous replacement of liquid on vapor. In this case, $\cos\theta$ is positive and the value of contact angle is between 0 and 90 °, shown in Figure 1.1 (a). On the contrary, if the surface tension between the solid-vapor is smaller than the surface tension between the solid-liquid, the $\cos\theta$ is negative and the value of contact angle is between 90 ° and 180 °, as shown in Figure 1.1 (b). When the wettability reaches its maximum limits, the contact angle value is closed to zero.

Wetting of textiles involves several primary processes, as shown in Figure 1.2: (a)

immersion of a solid in a liquid, (b) capillary sorption, (c) adhesion between a liquid and a solid and (d) spreading of liquid on the solid [11]. During immersion or capillary sorption, a solid-vapor interface disappears and a solid-liquid interface appears. When a liquid drop is placed on fabric, it will spread under capillary forces [12].

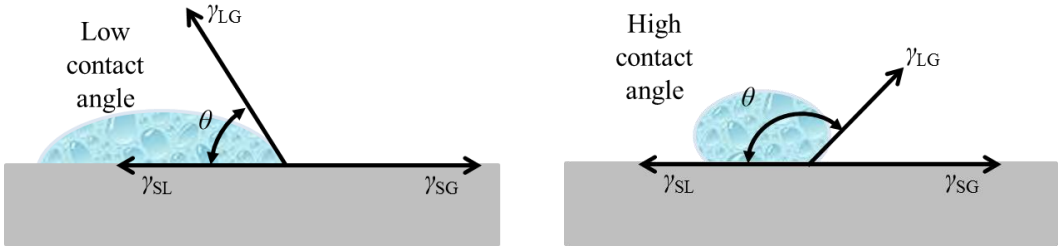

(a) (b)

Figure 1.1 Equilibrium state of a liquid drop on a solid surface: (a) contact angle between 0 and 90 °; (b) contact angle between 90 °and 180 °.

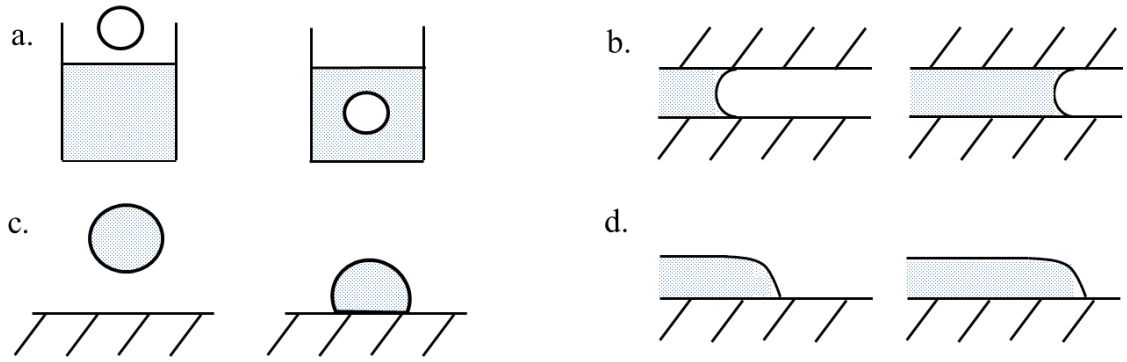

Figure 1.2 Wetting phenomena: (a) immersion; (b) capillary sorption; (c) adhesion; (d) spreading.

1.1.2 Wicking

The transport of a liquid into a fibrous substrate, such as yarn or fabric, may be caused by external forces or by capillary forces only. Wicking can only occur when fibers assembled with capillary spaces between them are wetted by a liquid. It can be visualized as a spontaneous displacement of a solid-air interface with a solid-liquid

interface in a capillary system [5].

In a simple case, such interface across the capillary is very small relative to the area of the wetted capillary wall and does not change during wicking. Hence, the only considerable change is the increase of the solid-liquid interface and decrease of the solid-air interface. For the process to be spontaneous, free energy has to be gained and the work of penetration has to be positive [5]. This is the case when the interfacial energy of the fiber surface in contact with vapor (air) γ_{SV} exceeds the interfacial energy between the liquid and the fiber surface γ_{SL}:

$$W_P = \gamma_{SV} - \gamma_{SL} = \gamma_{LV}\cos\theta, \tag{1.2}$$

where W_P is a measure of the energy required for capillary penetration.

Figure 1.3 shows the simplest case of wicking in a single capillary tube. The surface tension of the liquid causes a pressure difference across the curved liquid-vapor interface. The value for the pressure difference of a spherical surface was deduced in 1805 independently by Thomas Young (1773-1829) and Pierre Simon de Laplace (1749-1827), and is represented with the so called Young-Laplace equation [13, 14]:

$$\Delta P = \gamma_{LV}\left(\frac{1}{R'_1} + \frac{1}{R'_2}\right). \tag{1.3}$$

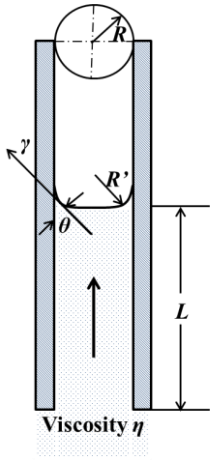

Figure 1.3 Wicking in a capillary system.

For a capillary with a circular cross section, the radii of the curved interface R'_1 and R'_2 are equal. Therefore,

$$\Delta P = 2\gamma_{LV} / R' . \tag{1.4}$$

Here, $R' = R / \cos\theta$. (1.5)

R is the capillary radius. As the capillary spaces in a fibrous assembly are not uniform, the effective capillary radius R_e is used.

1.2 Wicking processes and mechanisms

1.2.1 Wicking processes

Wicking occurs when a fabric is completely or partially immersed in a liquid or in contact with a limited amount of liquid, such as a drop placed on the fabric. Capillary penetration of a liquid can therefore occur from an infinite (unlimited) or limited (finite) reservoir. Wicking processes from an infinite reservoir are immersion, transplanar wicking, and longitudinal wicking. Wicking from a limited reservoir is exemplified by a drop placed onto the fabric surface [5].

(1) Wicking from an infinite reservoir

Capillary penetration of a liquid from an infinite reservoir has been the subject of numerous studies [3, 15-23]. The wicking process and methods of measurement of wicking from an infinite reservoir are listed below:

(a) Immersion: Wicking during immersion occurs when the fabric or fibrous assembly in general is completely immersed in a liquid and the liquid enters the fabric from all directions [24]. It is a method for measuring the total amount of water that a fabric will absorb. In the test, weighed samples of the fabric are immersed in water for a given length of time, taken out and the excess water removed by shaking. They are then weighed again and the weight of water absorbed is calculated as a percentage of the dry weight of the fabric [1].

(b) Longitudinal or In-plane Wicking [5, 6]: Longitudinal wicking from an infinite reservoir occurs when the fabric is partially immersed in a large volume of liquid that can wet the fabric. It is always using the in-plane wicking measurements to evaluate the

absorbing power or liquid transport capabilities of fibrous sheet materials. Usually the distance covered by the liquid front or the amount of liquid absorbed per weight or surface area of the substrate is measured.

(c) Transplanar or Transverse Wicking: Transplanar or transverse wicking is the term used when the transmission of a liquid is through the thickness of the fabric, which is perpendicular to the plane of the fabric. Sorption of water in a towel is one practical example. [5, 7, 25]. It is also termed “demand wetting” [26] or “spontaneous transplanar liquid uptake” [27]. Transverse wicking is more difficult to measure than longitudinal wicking as the distances involved are very small and hence the time taken to traverse the thickness of the fabric is short [1].

(2) Wicking from a limited (finite) reservoir

The capillary penetration of a drop indicates several important properties of a textile fabric, including repellency [12], absorbency, sorption of stain, and stain resistance. Either the drop absorbency time [7, 28] or the spreading rate of the liquid within the fabric is measured [29-32]. Wicking of minute drops of liquid has become very important for printing technology [33] Wicking of a limited amount of liquid, such as a drop placed onto the surface of a textile fabric, is a more complicated process than wicking from an infinite reservoir [31].

1.2.2 Wicking mechanisms

Based on the extent of interactions with fibers, each of the four wicking processes can be divided into four categories [5]:

(1) Wicking of a liquid- no significant diffusion into the fiber surface. Such as a

hydrocarbon oil wicking into a polyester fabric at ambient temperature. Capillary penetration is the only process operating.

(2) Wicking accompanied by diffusion of the liquid into fibers or into a finish on the fiber. Such as water wicking in a cotton fabric and diffusing into fibers, water wicking into a soil-release treated polyester fabric, and diffusing into the finish. Two simultaneous processes are operating- capillary penetration and diffusion of the liquid into the fibers.

(3) Wicking accompanied by adsorption on fibers. Such as an aqueous surfactant solution wicking into a polyester fabric. Several processes are operating simultaneously -capillary penetration of the liquid, diffusion of the surfactant in the liquid, and adsorption of the surfactant on fibers.

(4) Wicking involving adsorption and diffusion into fibers. Such as an aqueous surfactant solution wicking into a cotton fabric. Several processes are operating simultaneously -capillary penetration, diffusion of the liquid into the fibers, diffusion of the surfactant in the liquid, and adsorption of the surfactant on the fibers.

1.3 Previous study on the liquid transport within fabrics

Until now, there are many studies on the liquid transport within fabrics, especially the wetting and wicking in fabrics. Researches on the wetting and wicking were focused on the measurement methods and the wetting and wicking process within porous substrate, including fibers, yarns, fabrics and so on.

For the previous study of the measurement methods, the BS 3424 method [34] specified a very long time period (24 hours) and was intended for coated fabrics with very low wicking properties. DIN 53924 [35] or Byreck method [36] specified a much shorter time of 5 minutes maximum and was therefore more relevant to the studies of clothing comfort involving the transfer of perspiration. P.R. Harnett et al [7] presented a critical survey of the laboratory test methods used to measure wicking, and compared the four main methods (strip test, plate test, spot test and syphon test) through application to a range of knitted fabrics produced from various fiber types. They found that combination of methods provides a meaningful assessment of fabric wicking properties in the context of clothing comfort studies. Y.K. Kamath et al [37] designed an apparatus to electronically determine the time required for a liquid to wick horizontally into a certain length of yarn spontaneously. Anne Perwuelz et al [38] designed a technique based on the analysis of CCD images taken during the capillary rise of colored liquid in yarns, and studied the capillary flow in polyester and polyamide yarns and glass fibers. Mohamed Hamdaoui et al [39] studied the liquid transport and movement in yarns, using an experimental system based on the analysis of CCD images taken during the capillary rise of a colored liquid in the yarn. Kurt L. Adams [40] presented a technique that quantifies the in-plane flow properties of fibrous networks.

The technique was to monitor the shape of the advancing front of liquid as a function time. M. Howaldt [41] described a laser-doppler anemometer system which could provide quantitative information about the actual dynamic transport processes occurring within the fibrous assembly. You-Lo Hsieh [42] measured the liquid rise and capillary force in a capillary with a microbalance. The measurement was carried out by vertically connecting a capillary to the microbalance, raising a liquid upward to contact the lower end of the capillary and allowing wetting and wicking to occur. At equilibrium, the force detected by the balance reading was the sum of the external and the internal surface attraction forces. Paul Van Der Meeren et al [43] developed a radial, horizontal wicking experiment to determine the maximum absorption capacity of the fabric and quantify the wicking rate. Tokuzo Kawase et al [29] investigated the capillary spreading of a liquid drop in fabric by a photographic technique as a function of time, drop volume, and surface tension/viscosity ratio. Moreover, Tokuzo Kawase et al [44] applied an image analyzer (IA) technique to achieve a rapid, accurate, and especially objective measurement of spreading areas. F. Memariyan et al [45] also used the image analysis to measure the wicking of thin layer textiles. Xiao Chen et al [46] used the tensiometer to measure the capillary flow in nonwovens based on vertical wicking. Hiraku Ito et al [47] developed a new experimental apparatus, using the electrical capacitance technique to detect the small amount of water travelling along fibers. V Ramesh Babu et al [48] used a technique based on electrical open and closed circuit principle to measure the vertical capillary height of the liquid in fabrics as the function of time. M. Mazloumpour et al [49] developed an apparatus for measuring the wicking rise of water in fabric. The method was based on the electromagnetic field induction due to wicking penetration of water into capillary spaces of fabric samples. Ishizawa

Hiroaki et al [50] described the near-infrared spectral image measurement system for water transferences of woven fabrics. Morihiro Yoneda et al [51] developed a dew sensor array method to measure the in-plane capillary water flow in various types of woven fabrics.

In addition to developing the new methods of wicking for fabrics, there are many researches on the liquid transport properties reported previously. P.R. Load [52]carried out a comparison of the relative moisture uptake characteristics of ring and open-end yarns. Merve Kucukali Ozturk et al [53] investigated the wicking properties of cotton-acrylic rotor yarns and knitted fabrics, and discussed the effect of yarn wicking on wicking of fabric in both wale and course directions. The results showed that wicking abilities of yarns and fabrics increased with the increase in acrylic content in the blends and with the use of thicker yarns. Moreover, they found that yarn wicking had a significant effect on fabric wicking. Esra Coskuntuna et al [54] designed two different fibrous structures with anisotropic wicking properties and developed wicking models for these structures. Meltem Yanilmaz et al [55] investigated the relationship between different knitted structures and some thermophysiological comfort parameters. They investigated the wetting, wicking and drying properties of slack and tight knitted fabrics, and calculated wicking parameters. The results showed that all tight knitted structures had higher contact angles than their slack forms due to higher compactness of the surface. Moreover, they found the parameters of comfort were significantly affected by knitted structure.

1.4 The purpose of this study

As described previously, it is well-known that the wetting and wicking properties of fabrics have an important effect on the liquid transport of fabrics in several fields of usages, such as clothes, dyeing, and paper and so on.

The liquid transport through clothes is always accompanied with temperature changes. For human body, the temperature changes will have an important effect on the comfort of clothes, especially during exercise or in rainy days. Therefore, it is necessary to measure both temperature and liquid transport in fabrics. However, there is little suitable method for measuring both of them continuously. Moreover, the water content of fabric is important in the thermal sensation of human body, which needs to be investigated. Furthermore, among the previous studies, the measuring methods of the wetting and wicking properties can be used only for pieces of fabric samples in static condition. There are no practical methods for measuring these properties in wearing clothes or other textile products in use.

The purpose of this study is:

(1) To develop a new method which can measure both temperature and liquid transport of multipoint on fabrics to investigate in detail the conditions when a droplet of liquid comes into contact with a fabric.

(2) To propose a new measurement method for in-plane capillary liquid flow, which can be used for estimating the liquid content of fabric in wearing.

(3) To investigate the effects of wicking property index (wicking coefficient) to establish predicting wicking coefficient of fabric from fabric structure.

1.5 Composition of this study

In this study, new methods were proposed for wicking measurement within fabrics in case of a limited reservoir and an unlimited reservoir.

In Chapter 2, the wicking theory and the measurement method used in this study are proposed. T-type thermocouples are used and the verification of this kind of temperature sensor is described.

In Chapter 3, a multipoint thermocouple-equipped fabric for temperature measurement was developed and used to measure both temperature and liquid transport during the wetting and drying process. The possibility of the thermocouple was verified. Temperature distribution caused by diffusion and evaporation at different relative humidity was discussed. Moreover, a two-layer thermocouple-equipped fabric was woven, which can be used as garments for temperature measurement in the future.

In Chapter 4, a new thermocouple array method was proposed for measuring in-plane capillary water flow. Compared the results with the data acquired using the horizontal Byreck method (DIN 53924), the thermocouple method was found to be suitable for automatic and precise measurement of in-plane capillary water flow within fabrics. Moreover, based on this method, the feasibility of predicting the water contents of fabrics from temperature differences generated during the flow process was also investigated.

In Chapter 5, based on the measurement method introduced in Chapter 4, the relationship between wicking coefficients of fabrics and yarns was investigated from a range of plain fabrics, woven by varying the yarn kind (fiber content), yarn count and

weave density.

Finally, in Chapter 6, the conclusion of this study is described.

References:

[1] B P Saville. Physical testing of textiles. The Textile Institute, 2000.

[2] Parson K. Human thermal environments: The effects of hot, moderate and cold environments on human health, comfort and performance (Second edition). CVC Press, 2002. P. 156-195.

[3] You-Lo Hsieh, Bangling Yu and Mary Michelle Hartzell, Liquid wetting, transport, and retention properties of fibrous assemblies: Part II: Water wetting and retention of 100% and blended woven fabrics. *Text. Res. J.* 1992; 62 (12): 697-704.

[4] Rita M. Crow. Moisture, liquid and textiles: A critical review. Defence research establishment Ottawa, 1987.

[5] Erik Kissa, Wetting and wicking. *Text. Res. J.* 1996; 66 (10): 660-668.

[6] A. Patnaik, R. S. Rengasamy, V. K. Kothari et al, Wetting and wicking in fibrous materials. *Text. Prog.* 2010; 38 (1) : 1-105.

[7] P. R. Harnett, P. N. Mehta, A survey and comparison of laboratory test methods for measuring wicking. *Text. Res. J.* 1984; 54 (7): 471-478.

[8] Chureerat Prahsarn, Factors influencing liquid and moisture vapor transport in knit fabrics, Doctor's dissertation, North Carolina State University, 2001, pp12.

[9] Arthur W. Adamson, Irene Ling, The status of contact angle as a thermodynamic property. *Adv. Chem.* 1964; 43: 57-73.

[10] Bernard Miller, Raymond A. Young, Methodology for studying the wettability of filaments. *Text. Res. J.* 1975; 45: 359-365.

[11] Repellent finishes in Handbook of Fiber Science and Technology, Part II B (edited by B.M. Lewin and S.B. Sello), Marcel Dekker, New York, USA, 1984, p. 144.

[12] Erik Kissa, Handbook of fiber science and technology, Part II B (edited by B. M.

Lewin and S. B. Sello), Marcel Dekker, New York, USA, 1984.

[13] J. Pellicer, V. Garcia-Morales and M. J. Hernandez, On the demonstration of the Young-Laplace equation in introductory physics courses. *Phys. Educ.* 2000; 35 (2): 126-129.

[14] E. Hernandez-Baltazar, J. Gracia-Fadrique, Elliptic solution to the Young-Laplace differential equation. *J Colloid and Interface Sci.* 2005; 287: 213-216.

[15] You-Lo Hsieh, Bangling Yu, Liquid wetting, transport, and retention properties of fibrous assemblies: Part I: Water wetting properties of woven fabrics and their constituent single fibers. *Text. Res. J.* 1992; 62 (11): 677-685.

[16] George L. Batten JR, Liquid imbibition in capillaries and packed beds. *J Colloid and Interface Sci.* 1984; 102 (2): 513-518.

[17] Kazuhiko Kurematsu, Masumi Koishi, Kinetic studies on liquid penetration in polyester nonwoven fabric. *J Colloid and Interface Sci.* 1984; 101 (1): 37-45.

[18] Mario F Letelier S, Hans J Leutheusser, Refined mathematical analysis of the capillary penetration problem. *J Colloid and Interface Sci.* 1979; 72 (3): 465-470

[19] J Szekely, A W Neumann, Y K Chuang, The rate of capillary penetration and the applicability of the Washburn equation. *J Colloid and Interface Sci.* 1971; 35 (2): 273-278.

[20] Dganit Danino, Abraham Marmur, Radial capillary penetration into paper: limited and unlimited liquid reservoirs. *J Colloid and Interface Sci.* 1994; 166: 245-250.

[21] A. Borhan, K. K. Rungta, An experimental study of the radial penetration of liquids in thin porous substrates. *J Colloid and Interface Sci.* 1993; 158: 403-411.

[22] Abraham Marmur, The radial capillary. *J Colloid and Interface Sci.* 1988; 124 (1): 301-308.

[23] Abraham Marmur, Penetration of a small drop into a capillary. *J Colloid and Interface Sci.* 1988; 122 (1): 209-219.

[24] John R. McLaughlin, Mary E. Trounson, Rex . Stewart and A. John McKinnon, Surfactant solution transport in wool yarn: Part III: Immersion absorption. *Text. Res. J.* 1988; 58: 501-506.

[25] Brojeswari Das, A. Das, V.K. Kothari, R. Fangueiro, M. de Araujo. Moisture transmission through textiles Part II: Evaluation methods and mathematical modeling. *Autex Research Journal* 2007; 7 (3): 194-216.

[26] Lichstein B M. Demand wettability, a new method for measuring absorbency characteristics of fabrics. INDA Technical Symposium- Nonwoven Product Technology, Washington DC, 1974: 129-142.

[27] B. Miller, I. Tyomkin. Spontaneous transplanar uptake of liquids by fabrics. *Text. Res. J.* 1984; 54: 706-712.

[28] N.R. Bertoniere, S.P. Rowland. Spreading and imbibition of durable press reagent solutions in cotton-containing fabrics. *Text. Res. J.* 1985; 55 (1): 57-64.

[29] Tokuzo Kawase, Sakiko Sekoguchi, Tomiko Fujii, Motoi Minagawa. Spreading of liquids in textile assemblies: Part I: Capillary spreading of liquids. *Text. Res. J.* 1986; 56: 409-414.

[30] T. Gillespie. The spreading of low vapor pressure liquids in paper. *J. Colloid Sci.* 1958; 13: 32-50.

[31] Erik Kissa. Wetting and detergency. *Pure Appl. Chem.* 1981; 53 (11): 2255-2268.

[32] Elaine E. Clulow. Comparison of methods of measuring wettability of fabrics, and inter-laboratory trials on the method chosen. *J Text Inst* 1969; 60 (1): 14-28.

[33] J.F. Oliver, L. Agbezuge, K. Woodcock. A diffusion approach for modeling

penetration of aqueous liquids into paper. *Colloids Surf. A* 1994; 89: 213-226.

[34] BS 3424: Part 18: 1986. Methods for determination of resistance to wicking and lateral leakage to air. British Standards Institution, London.

[35] Din 53924. Velocity of suction of textile fabrics in respect of water- method determining the rising height. Berlin: Deutsches Institut fur Normung, 1997.

[36] Japanese Industrial Standard L 1907: 1994. Test method of water absorbency of textiles-5.1.2, Byreck method.

[37] Y.K. Kamath, S.B. Hornby, H.D. Weigmann, M.F. Wilde. Wicking of spin finishes and related liquids into continuous filament yanrs. *Text. Res. J.* 1994; 64 (1): 33-40.

[38] Anne Perwuelz, Pascal Mondon, Claude Caze. Experimental study of capillary flow in yarns. *Text. Res. J.* 2000; 70 (4): 333-339.

[39] Mohamed Hamdaoui, Faten Fayala, Sassi Ben Nasrallah. Dynamics of capillary rise in yarns: Influence of fiber and liquid characteristics. *J. Appl. Polym. Sci.* 2007; 104: 3050-3056.

[40] Kurt L. Adams, Ludwig Rebenfeld. In-plane flow of fluids in fabrics: Structure/ flow characterization. *Text. Res. J.* 1987; 57: 647-657.

[41] M. Howaldt, A.P. Yoganathan. Laser-doppler anemometry to study fluid transport in fibrous assemblied. *Text. Res. J.* 1983; 53: 544-551.

[42] You-Lo Hsieh. Liquid transport in fabric structures. *Text. Res. J.* 1995; 65 (5): 299-307.

[43] Paul Van Der Meeren, Jan Cocquyt, Silvia Flores, Hugo Demeyere and Marc Declercq. Quantifying wetting and wicking phenomena in cotton terry as affected by fabric conditioner. *Text. Res. J.* 2002; 72 (5): 423-428.

[44] Tokuzo Kawase, Sakiko Sekoguchi, Tomiko Fujii and Motoi Minagawa. Spreading

of liquids in textile assemblies: Part III: Application of an image analyzer system to capillary spreading of liquids. *Text. Res. J.* 1988; 58: 306-308.

[45] F. Memariyan, E. Ekhtiyari. Study on wicking measurement in thin layer textiles by processing digital images. *IJE Transactions A: Basics* 2010; 23 (1): 101-108.

[46] Xiao Chen, Philippe Vroman, Maryline Lewandowski, Anne Perwuelz and Yan Zhang. Study of the influence of fiber diameter and fiber blending on liquid absorption inside nonwoven structures. *Text. Res. J.* 2009; 79 (15): 1364-1370.

[47] Hiraku Ito, Yoichiro Muraoka. Water transport along textile fibers as measured by an electrical capacitance technique. *Text. Res. J.* 1993; 63 (7): 414-420.

[48] V Ramesh Babu, C V Koushik. Capillary rise in woven fabrics by electrical principle. *Indian J Fibre Text Res* 2011; 36: 99-102.

[49] M. Mazloumpour, F. Rahmani, N. Ansari, H. Nosrati and A.H. Rezaei. Study of wicking behavior of water on woven fabric using magnetic induction technique. *J Text Inst* 2011; 102 (7): 559-567.

[50] Ishizawa Hiroaki, Yotsuda Toyokazu, Kanai Hiroyuki, Nishimatsu Toyonori and Toba Eiji. Estimation of water transfer in woven fabrics using near-infrared spectral image. *Journal of the Textile Machinery Society of Japan* 2004; 57 (7): 41-46.

[51] Morihiro Yoneda, Masako Niwa. Measurement of in-plane capillary water flow of fabrics. *Sen-I Gakkaishi* 1992; 48 (6): 288-298.

[52] P.R. Load. A comparison of the performance of open-end and ring spun yarns in terry toweling. *Text. Res. J.* 1974; 44: 516-522.

[53] Merve Kucukali Ozturk, Banu Nergis and Cevza Candan. A study of wicking properties of cotton-acrylic yarns and knitted fabrics. *Text. Res. J.* 2011; 81 (3): 324-328.

[54] Esra Coskuntuna, Alex J. Fowler and Steven B. Warner. Fibrous structures with designed wicking properties. *Text. Res. J.* 2007; 77 (4): 256-264.

[55] Meltem Yanilmaz, Fatma Kalaoglu. Investigation of wicking, wetting and drying properites of acrylic knitted fabrics. *Text. Res. J.* 2012; 82 (8): 820-831.

Chapter 2

Wicking theory and measurement method

Chapter 2 Wicking theory and measurement method

2.1 Wicking theory

Liquid transfer mechanisms include water diffusion and capillary wicking, which are determined mainly by effective capillary pore distribution, pathway and surface tension [1]. Wicking is the spontaneous flow of a liquid in a porous substance, driven by capillary forces. It takes place only in wet fabrics or when fabrics come into contact with water, and the contact angle determines their wicking behavior. Wicking is essential to the function of many products, including toweling, paper tissue, absorbent dressings and a variety of absorbent hygiene products [2]. It is commonly described by the theory of Lucas [3] and Washburm [4], which modeled the porous medium as a bundle of cylindrical capillary tubes. Washburn proposed the well-known Lucas-Washburn kinetics equation to describe the relationship between wicking length and wicking time.

The liquid flow in a pipe is shown in Figure 2.1. On the assumption that the fluid is incompressible and Newtonian, the flow is laminar through a pipe of constant circular cross-section that is substantially longer than its diameter, and there is no acceleration of fluid in the pipe, the Poiseuille's equation [5, 6] is given by Equation (2.1):

$$Q = \frac{dV}{dt} = \frac{\pi R^4 \Delta P}{8\eta L}, \tag{2.1}$$

where, Q is the volume flow rate, V is the volume flow, t is time, η is the viscosity of a fluid, R is the radius of the pipe, L is the length of the liquid, and ΔP is the

pressure difference. The volume flow V is calculated as

$$V = \pi R^2 L . \tag{2.2}$$

Therefore,

$$\frac{dL}{dt} = \frac{R^2 \Delta P}{8\eta L} . \tag{2.3}$$

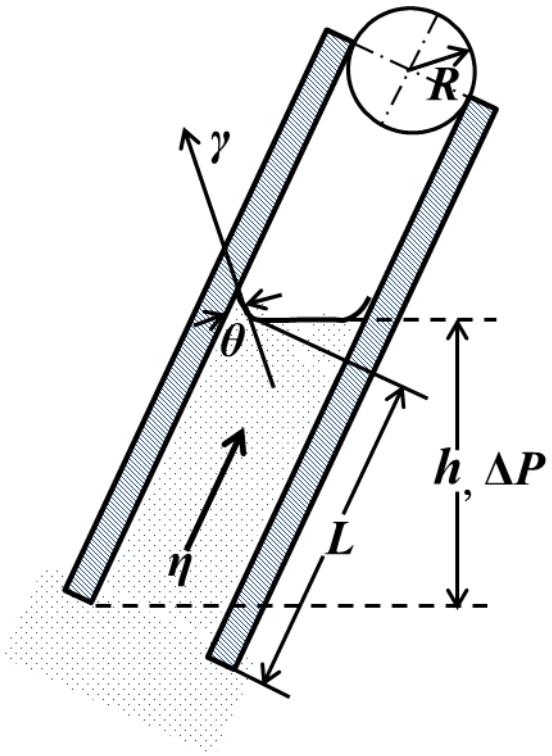

Figure 2.1 Capillary action.

Based on the Young-Laplace equation [7], the capillary pressure is calculated taking the gravity into account, as shown in Equation (2.4).

$$\Delta P = \frac{2\gamma \cos\theta}{R} - \rho g h. \tag{2.4}$$

Here, γ is the liquid-vapor surface tension, θ is the contact angle of the solid-liquid

system, ρ is the volume density of fluid, g is the gravitational acceleration, and h is the capillary rise.

Integrating Equation (2.3) with initial condition of L=0 at t=0, and substituting Equation (2.4) for ΔP, Equation (2.5) can be obtained.

$$L^2 = \frac{R^2}{4\eta}\left(\frac{2\gamma\cos\theta}{R} - \rho g h\right)t. \tag{2.5}$$

Equation (2.5) shows the relationship between wicking length and wicking time. In order to simplify the calculation, the Newtonian liquid was assumed, which completely wet and dry capillary tube. Furthermore, considering the radius of the capillary is so small that the meniscus is spherical at all times, so that the gravity effects can be neglected [8] and Equation (2.5) can be written as the Lucas-Washburn equation:

$$L = \left(\frac{R\gamma\cos\theta}{2\eta}\right)^{1/2} t^{1/2}. \tag{2.6}$$

As the kinetics of wicking in textiles is critical in many applications, it is often investigated by fitting the experimental data to the Lucas-Washburn equation [9]. According to Equation (2.6), a plot of L versus $t^{1/2}$ should be linear and pass through the origin. The slope of the line, referred to the wicking coefficients W, is given by Equation (2.7) and is determined by fitting experimental data to Equation (2.6).

$$W = (R\gamma\cos\theta/2\eta)^{1/2}. \tag{2.7}$$

That is to say, the wicking coefficient at which a liquid penetrates any capillary (or any capillary with a small surface) under its own capillary pressure is directly

proportional to the radius of the capillary, the cosine of contact angle, and the surface tension and inversely proportional to the viscosity of the liquid.

2.2 Measurement method used in this study

2.2.1 Measurement theory

During the water transport of fabric, because of absorption, diffusion and evaporation, fabric temperature changes accompanying with heat transmission. The fabric temperature is determined by the heat changes (generation or loss) during the water transport process. Neglect heat of radiation and convection, the net heat (Q) can be calculated based on Figure 2.8.

$$Q = Q_a - Q_e, \tag{2.8}$$

where Q_a is the generated heat produced by water adsorption, Q_e is the heat consumption due to water evaporation.

At a constant temperature and relative humidity, if a drop of water drops on fabric, heat is generated because of water adsorption (Q_a), however, evaporation heat (Q_e) is 0 at first, therefore, the total heat Q is larger than 0, and the temperature will increase until complete absorption. With the water transfer, evaporation happens and the heat consumption is larger than the adsorption heat (Q_a), and the temperature will fall down. Finally, the evaporation decreases then temperature returns to environment temperature. Therefore, in order to develop a method which can measure both temperature and liquid transport in fabrics, a temperature sensor method was proposed, as the temperature sensor can measure fabric temperature any time in the wetting and drying process.

For example, if a fabric is placed at a constant environment consisted of ambient temperature and relative humidity, when a drop of water with the same temperature dropped on this fabric, the temperature of the fabric changed because of heat

transference associated with both wetting and evaporation.

2.2.2 Temperature sensor used in this study

There are many kinds of temperature sensors. The thermometer is commonly used for measuring temperature of body, liquid and so on. However, it is inconvenient as it cannot provide real-time temperature information. The infrared thermal imaging thermometry has many advantages, such as high speed, large area, non-contact measurement and so on. However, it can only measure surface temperature and the precision of the measurement is influenced by many factors, including emissive and reflectivity of an object surface, ambient temperature, atmospheric temperature, measuring distance and so on [10]. Resistance temperature detector, integrated circuit (IC) temperature sensor and thermocouple are electrical thermometer with high reliability. As one of the highly reliable temperature sensors, thermocouples are preferred due to their wide operation range, low cost and fast response time [11]. Therefore, in this study, thermocouples were used to measure temperature.

The Seebeck effect, shown in Figure 2.2, is a phenomenon in which temperature difference between two dissimilar electrical conductors or semiconductors (A and B in Figure 2.2) produces a voltage difference between the two substances. It also refers to the thermoelectric effect in which a voltage is generated by a temperature gradient due to the movement of charge carriers from the higher temperature point to the lower temperature point [12]. Different sets of two substances, called thermocouples, are generally used as temperature sensors. The voltage occurred at two points, is called thermal electromotive force. It does not depend on a specific arrangement of the materials, nor on a specific way of joining them [13].

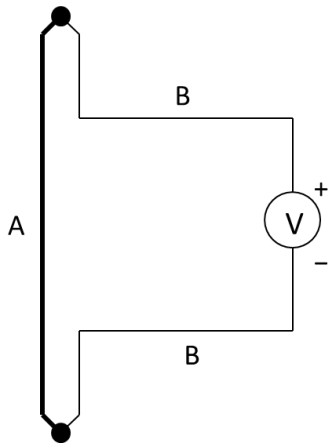

Figure 2.2 The Seebeck effect.

There are many types of thermocouples [14], such as B-type, R-type, S-type, N-type, K-type, E-type, J-type and T-type and so on. They are different for the two substances of A and B in Figure 2.2, and are usually selected on the basis of the temperature range and sensitivity needed. The two substances are also called element wires. The T-type thermocouple, taking copper and constantan as element wires, is widely used for low temperature and precision measurement. The standard temperature range is from -200 ℃ to 350 ℃, and the accuracy of the thermocouple is within 0.5 ℃.

On the basis of Seebeck effect, Stefan Ziegler et al [15] used conductive textile products to manufacture thermocouples and studied on the relationship between temperature differences and electromotive force differences. The thermocouples were made by metal fibers and metal fabrics and the size was large. Therefore, they cannot used to measure water transport within fabrics used for clothes.

If fabric contacts with water, the temperature of the fabric will change. Therefore, in this study, the thermocouples were used for temperature measurement and for measuring water transport on fabrics.

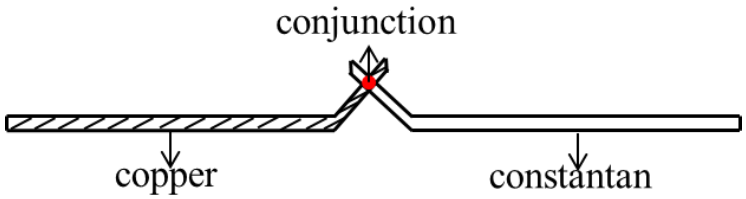

Figure 2.3 Structure of T-type thermocouple.

In this study, a T-type thermocouple was used, with element wires of 0.1 mm in diameter. The structure of the T-type thermocouple is shown in Figure 2.3. The end of copper and constantan wires were connected as a conjunction to form a measurement point. The mini-type spot welding machine (Kondo-technology), as shown in Figure 2.4 was used to welding the conjunction, with the volume of about 2. Based on the marks in Figure 2.4, conjunction can be made as follows: press “A” to turn on the machine, and then regulate the suitable voltage marked “B”, put the thermocouple element wires crosswise on the holder marked “C”, then press “D” to make a conjunction. As a measurement point, the conjunction can response the temperature changes. The other end of these element wires were free point for connecting with device for temperature measurement, shown in Figure 2.5 (KE3000, Chino Co.). The devices can be divided into three parts, the power supply unit, the communication unit and the input unit, as shown in Figure 2.5. The devices are relayed to and recorded by a computer, and it owns maximum 60 channels which can measure temperature of maximum 60 points simultaneously. The measured temperature was recorded and saved by software “KIDS-USB”, showing the measurement screen in Figure 2.6. In this figure, 24 channels were used.

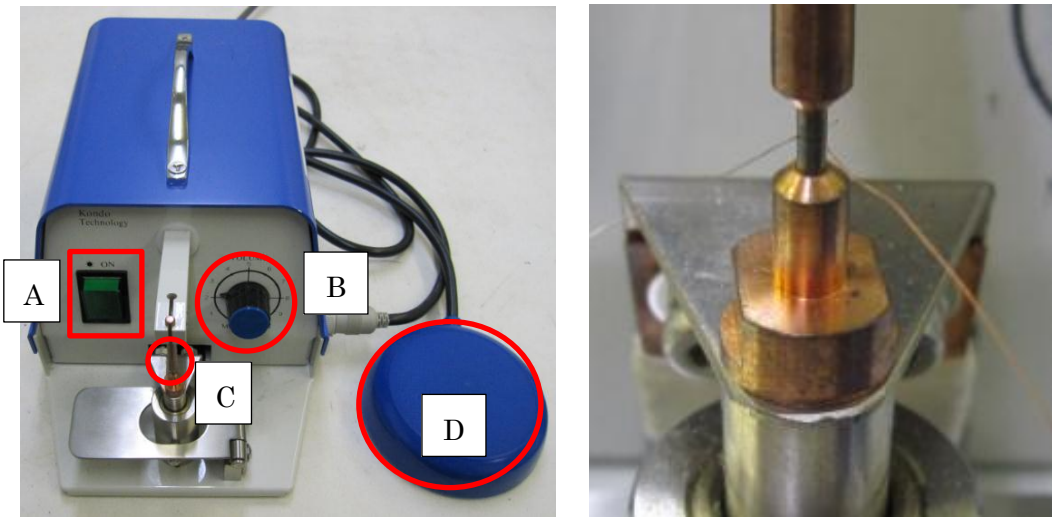

(a) (b)

Figure 2.4 The image of weld machine: (a) the weld machine (A. power; B. volume; C. holder; D. operating button); (b) the detail of Part C.

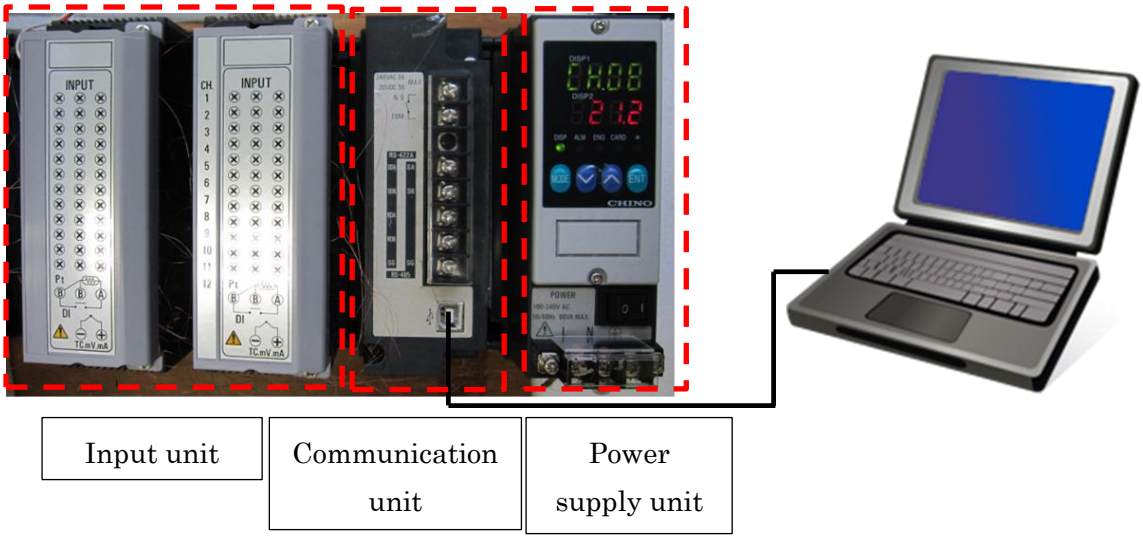

Figure 2.5 Temperature measurement devices relayed to a computer.

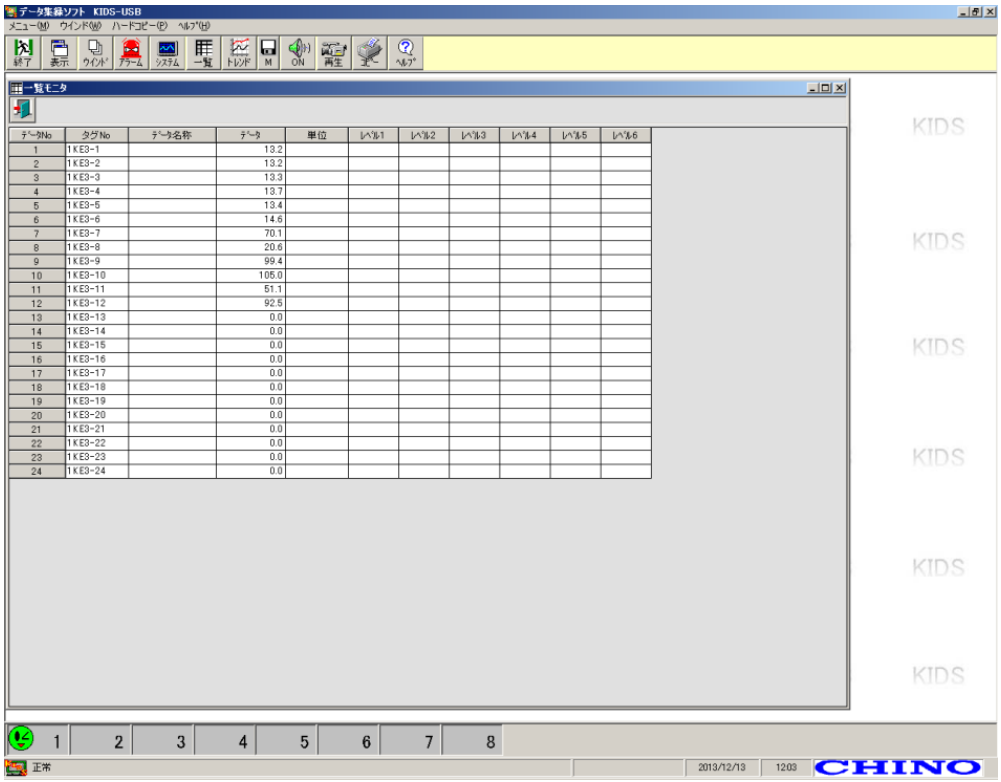

Figure 2.6 Interface of temperature recording and saving software.

2.2.3 Verification of commercial thermocouples

In this study, commercial temperature sensors (Chino Co.), made from copper and constantan, were used to verify the precision of man-made thermocouples, by comparing the measured temperature with temperature measured by commercial sensors. The commercial thermocouple is a kind of T-type sensor (Chino Co.), made with 0.32 diameter copper and constantan element wires and were factory calibrated. Therefore, in order to test and verify the precision of the commercial temperature sensors, the F100 Precision Handheld Thermometer (ASL Ltd) was used to measure temperature for comparing with the results measured by commercial sensors.

The F100 Precision Handheld Thermometer is a high precision instrument designed for laboratory, commercial and industrial temperature measurement and

calibration application, with accuracy of ±0.02 ℃ over a range of -200 ℃ to 850 ℃. The thermometer is operated with Pt100 (100Ω) Platinum Resistance Thermometers as probe and it has several features, including:

(1) Two input channels.

(2) A large graphic LCD display for excellent viewing of temperature measurement values and instrument settings.

(3) USB communication interface as standard for automated monitoring and calibration applications.

(4) Calibration against traceable external standards.

The experiment was carried out as follows:

(1) Measure temperature at constant environment conditions, by changing temperature from 10 ℃ to 30 ℃, at an interval of 1 ℃, then compare the temperature measured by thermocouples with F100 thermometer.

(2) Measure temperatures in a temperature-humidity chamber with temperature changes from 20 ℃ down to 15 ℃ and then return to 20 ℃ at 65% RH. Moreover, temperatures during these changes were also measured by the commercial temperature sensors and T-type thermocouple, and both the results were compared and discussed.

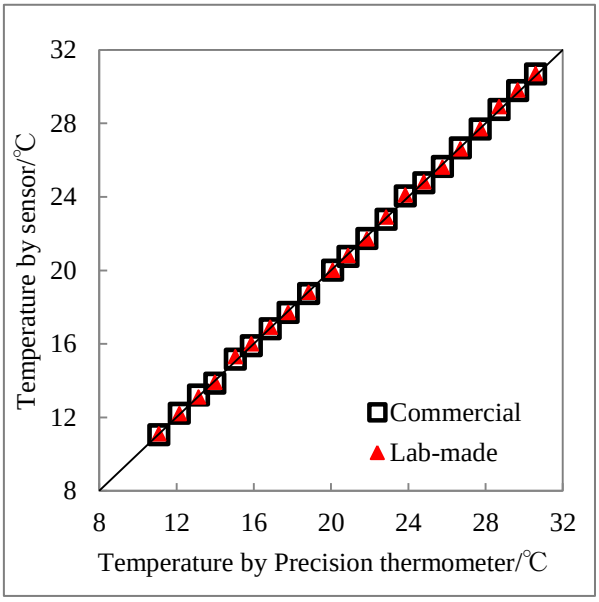

Figure 2.7 Temperature comparison measured by precision and commercial thermometer.

The result of experiment (1) was shown in Figure 2.7. The “Commercial” and “Thermocouple” represent the results measured by commercial thermocouple and self-produced thermocouple, and the “F100” is the comparative thermometer. The relationship of temperature between thermocouples and F100 thermometer shows straight line, which means at constant temperature, the measured values of F100 and commercial thermocouple and self-produced thermocouple are the same. Moreover, the result of experiment (2) was shown in Figure 2.8. It shows that during 90 minutes, the temperature measured by thermocouple is almost the same with temperatures measured by F100 Precision Handheld Thermometer (F100). During the increase and decrease of environment temperature, the measured temperature changes show the consistency between thermocouples and F100. Therefore, it can be concluded that the commercial thermocouples can be used for standard thermocouple to verify the man-made T-type

thermocouples.

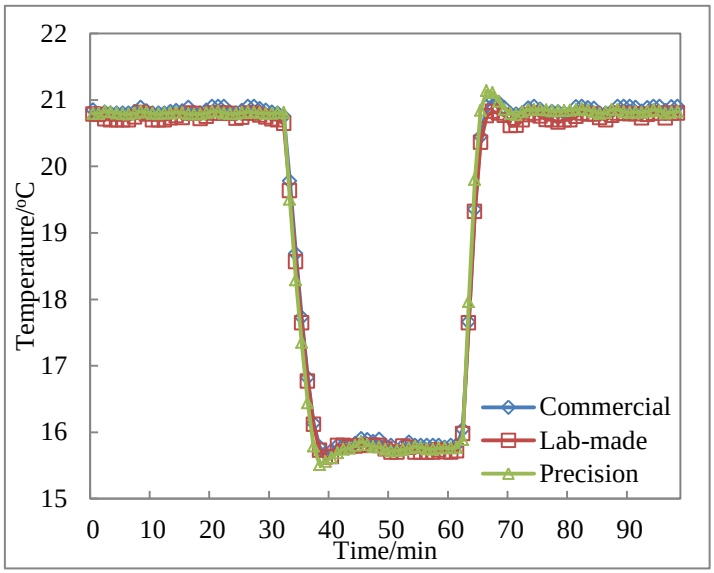

Figure 2.8 Temperature measured by T-type thermocouples and F100 Precision Handheld Thermometer.

References:

[1] R. Fangueiro, A. Filgueiras, F. Soutinho, Xie Meidi. Wicking behavior and drying capability of functional knitted fabrics. *Text. Res. J.* 2010; 80 (5): 1522-1530.

[2] Kevin T. Hodgson, John C Berg. The effect of surfactants on wicking flow in fiber networks. *J. Colloid Interface Sci.* 1988; 121 (1): 22-31.

[3] Richard Lucas. The time law of the capillary rise of liquids. *Kolloid Zeitschrift* 1918; 23 (1): 15-22.

[4] Edward W. Washburn. The dynamics of capillary flow. *Phys. Rev.* 1921; 17: 273-283.

[5] Tamura E, Zukai Hajimete No Ryuutai Rikigaku. Kagaku Tosho Edition, Tokyo. 2010.

[6] David Byar, Richard V. Fiddian, Marcia Quereau, John T. Hobbs, Edward A. Edwards. The fallacy of applying the Poiseuille equation to segmental arterial stenosis. *Am. Heart J.* 1965; 70 (2): 216-224.

[7] Paul C. Reeves, Michael A. Celia. A functional relationship between capillary pressure, saturation, and interfacial area as revealed by a pore-scale network model. *Water Resour. Res.* 1996; 32 (8): 2345-2358.

[8] P. Joos, P. Van Remoortere, M. Bracke. The kinetics of wetting in a capillary. *J. Colloid Interface Sci.* 1990; 136 (1): 189-197.

[9] Mhetre S and Parachuru R. The effect of fabric structure and yarn-to-yarn liquid migration on liquid transport in fabrics. *J. Text. Inst.* 2010; 101: 621-626.

[10] Shaosheng Dai, Xiaohui Yan, Tianqi Zhang. Study on high-precision temperature measurement of infrared thermal imager. *Infrared Phys. Technol.* 2010; 53: 396-398.

[11] K. Danisman, I. Dalkiran, F.V. Celebi. Design of a high precision temperature measurement system based on artificial neural network for different thermocouple types. *Measurement* 2006; 39: 695-700.

[12] Sihai Wen, D.D.L. Chung. Seebeck effect in steel fiber reinforced cement. *Cem. Concr. Res.* 2000; 30: 661-664.

[13] A W Van Herwaarden, P M Sarro. Thermal sensors based on the Seebeck effect. *Sens. Actuators* 1986; 10: 321-346.

[14] Japanese Industrial Standard C 1602: 1995. Thermocouples.

[15] Stefan Ziegler, Michal Frydrysiak. Initial research into the structure and working conditions of textile thermocouples. *Fibres Text. East. Eur.* 2009; 17 (6): 84-88.

Chapter 3

Change of temperature of cotton and polyester fabrics during wetting and drying

Chapter 3 Change of temperature of cotton and polyester fabrics during wetting and drying

3.1 Introduction

As a basic function of clothing, it is important to restrict heat loss from the body, especially in cold, rainy and some other climates. As the fabrics used in making apparel differ greatly in their moisture sorption and thermal properties, it is important to take these characteristics into account when choosing clothing for particular applications.

In practical terms, heat and moisture transfer properties of fabrics are especially significant, as they play an important role in determining the thermal comfort associated with wearing the materials. The thermal comfort of the wearer is dependent on the clothing relationship with the wearer, its activity and the environment, since garment can be an obstacle to the heat and moisture transfers [1].

Research into heat and moisture vapor transfer of textiles focuses on the equilibrium and transient conditions of moist fabrics during skin contact or fabric, and the influencing parameters, such as thickness and porosity of fabric [2-15]. Li et al. investigated the fiber moisture sorption behavior in the sensory perception of dampness in fabric experimentally and mechanistically [2]. Plante also carried out the dampness perception trials on the influence of fiber type, fabric moisture content, and ambient conditions on the subjective assessment of dampness in fabrics [3]. Alber-Wallerstrom [16] researched on the efficiency of sweat evaporation by a continuous weighing technique. Examining on the relationship between the thickness and thermal resistance of textile fabrics, a significant reduction in sweating evaporation efficiency was found

in subjects exercising in moderate, dry and humid heat. Heat transfers of underwear at low activity are mainly governed by conductive, convective and radiative heat transfer mechanisms [17]. At high activity levels or in warm conditions, evaporation becomes predominant [18]. Therefore, at high activity levels, the thermal sensation is mainly influenced by sweating rather than by skin surface temperature, since the evaporative cooling effect by the sweating allows maintaining skin temperature at a favorable level [19]. Moreover, A new test method had been developed based on the contact electrical resistance of fabric [20] [21]. However, because of the diffusion characteristics of liquid water, when rain or sweat impinges on a fabric there will be temperature differences over the surface of the material, and these will have an effect on the wearer's level of comfort. To properly understand the effects of moisture it is therefore necessary to investigate in detail the conditions that occur when a droplet of liquid comes into contact with a particular fabric.

Lyons and Vollers [22] analyzed the drying process of textile materials and identified three distinct stages. The first is an initial warm-up period that may or may not be significant in the overall process. The second stage is the constant drying rate period, in which the rate of vaporization balances the rate of heat transfer and the temperature of the saturated surface remains constant. The third stage is the falling rate period, during which moisture flow to the surface is insufficient to maintain saturation and the plane of evaporation moves into the fabric. Fibers in the fabric then begin to desorb moisture until equilibrium is reached between the fabric and the surrounding environment. In order to analyze the temperature of fabric during the drying process, we try to show the relationship between the temperature and water content during the wetting and drying process.

On the basis of Seebeck effect, Stefan Ziegler et al [23] used conductive textile products to manufacture thermocouples and studied the relationship between temperature differences and electromotive force differences. This work, however, was limited in its scope because it relied on thermocouples made of metal fibers and fabrics that were not suitable for wearable garments and water transport in fabrics.

As noted above, T-type thermocouples have been used on fabrics for temperature measurements based on the theory of the Seebeck effect. In order to discuss the water diffusion on fabric, and investigate temperature change of wetted fabrics, a multipoint thermocouple-equipped fabric had been fabricated. It could be used for on-line multipoint temperature measurement of the fabric on various conditions.

In this study, samples of intact fabric were laid over thermocouple-equipped specimens of the same material, following which the top fabric layer was wetted by the application of a droplet of water. The temperatures during wetting and drying process are measured between two fabrics by thermocouple sensors on fabric, and the relationship between temperature distribution and diffusion of water had been discussed. Moreover, the woven method for a two-layer thermocouple-equipped fabric was shown in this study.

3.2 Experimental

3.2.1 Manufacture of thermocouple-equipped fabric

Cotton and polyester woven fabrics were used to manufacture thermocouple-equipped fabrics, with basic specifications shown in Table 3.1.

T-type thermocouples were employed for temperature sensors, using ϕ0.1mm copper and constantan as element wires. The standard temperature range is from -200℃ to 350℃, and the accuracy of the thermocouple is within 0.5℃. The wires were first sewn into fabric along the warp direction, and the distance between a couple of element wires is about 1cm. After been sewn, the ends of each element wire were welded together to form a measurement point located on the surface of fabric. The device for welding was shown in Figure 2.4, Chapter 2. The point can measure room temperature, and inner temperature between fabrics by adjusting the spatial location of measurement point. The other hand of element wires is free point for connecting with device for temperature measurement. A schematic and a photograph of the thermocouple arrangement are provided in Figures 3.1 and 3.2.

Table 3.1 Specification of fabrics.

Fiber content	Yarn count	Weave	Density (cm^{-1})		Mass/unit area (g/m^2)	Thickness (mm)
			Warp	Weft		
100% Cotton (C)	28tex(21s)	Plain	27	22	153.52	0.852
100% Polyester (P)	28tex(2/40s), spun yarn	Double-layer	25	25	211.93	1.458

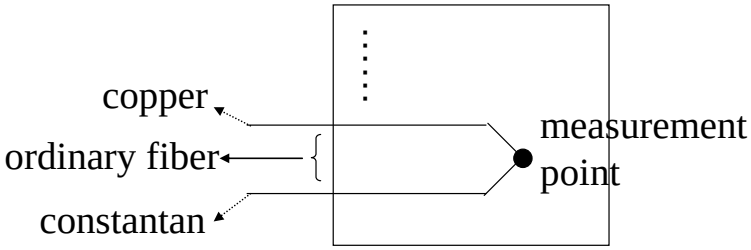

Figure 3.1 Basic structure of fabric thermocouple.

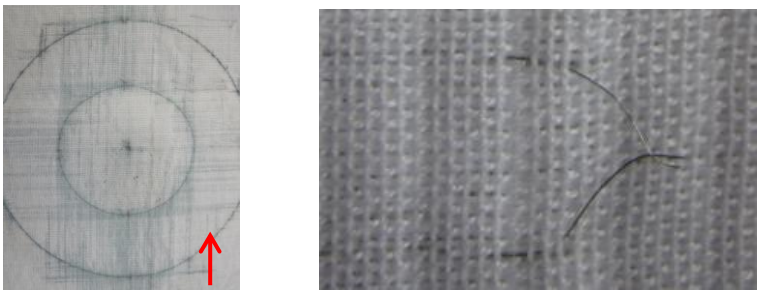

(a) (b)

Figure 3.2 Image of an actual fabric thermocouple: (a) the actual thermocouple-equipped polyester fabric; (b) detail of the temperature sensor.

In order to measure temperature variations of fabric during wetting and drying process, it has brought up an idea of multipoint thermocouple-equipped fabric, in which the thermocouple measurement points may be arranged to form various geometric shapes, such as circle, square. In this study, a pattern was used consisting of two concentric circles with radii of 3 and 6cm, with the measurement points located along the warp yarns as shown in Figure 3.3.

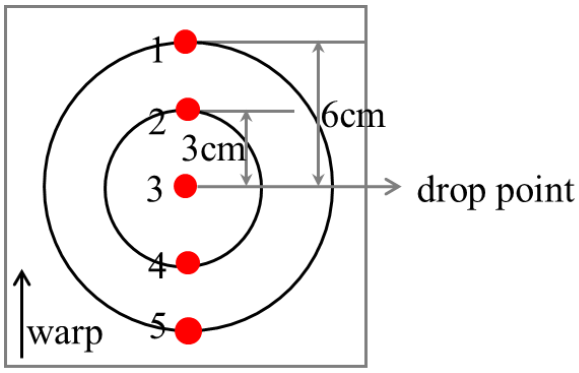

Figure 3.3 Multipoint thermocouple-equipped fabric, showing measurement points.

3.2.2 Temperature distribution measurements

(1) Validation of thermocouple fabric

After the measurement points had been welded and the free thermocouple leads connected to a data collection device (KE 3000, Chino Co.), shown in Figure 2.5, Chapter 2, the system was tested by using the thermocouple-equipped fabrics to measure room temperature. These measurements were recorded at constant ambient temperature and humidity, with the thermocouple measurement points arranged such that they were not contacting the fabric. A diagram of the test configuration is shown in Figure 3.4. Temperature data could be collected and recorded in a sampling rate of $0.2s^{-1}$, or 12 data points per minute automatically. In the meanwhile, in order to verify the validity of thermocouples in fabric, two commercial thermocouples were placed above the same fabric to measure room temperature and the measured temperatures were recorded by computer. The accuracy of commercial thermocouples were verified shown in Chapter 2, therefore, they could be used as standard sensors for comparison purposes. During the experiment work, the 12 data points acquired over each minute were averaged to give a single temperature value, T_{AVE}.

$$T_{AVE_n} = \frac{1}{12}(T_1 + T_2 + \cdots + T_m) \tag{3.1}$$

Where, T_{AVE} is the average temperature at n minute, m is 12.

Each temperature measurement trial was replicated three times.

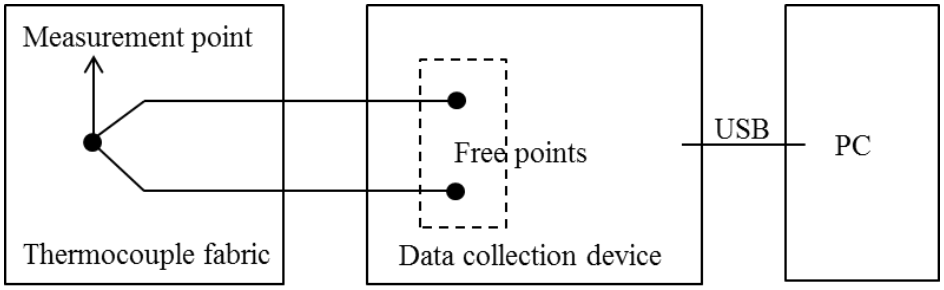

Figure 3.4 Schematic of temperature measurement instrumentation.

(2) Measurement of temperature distributions of wetted fabrics

Temperatures were measured by the thermocouples on fabric during the wetting and drying process when water was dropped, as shown in Figure 3.5.

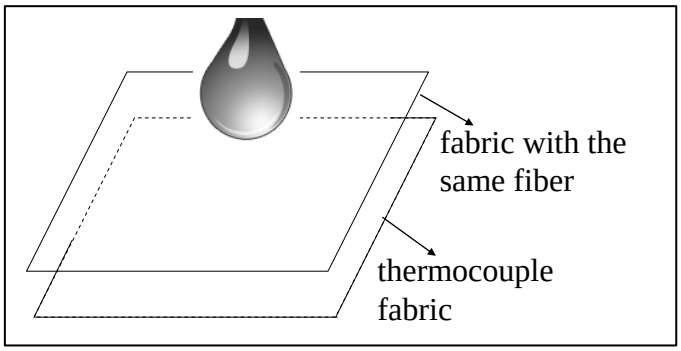

Figure 3.5 Diagram of the spot test.

To investigate the liquid transmission characteristics of fabrics, and the accompanying temperature changes, the spot test [25] was employed. In this test, a sample of the thermocouple-equipped fabric (fabric 1), a sample of the same fabric

without thermocouples (fabric 2) and a quantity of distilled water were all allowed to equilibrate to the ambient temperature of 20 ± 1 ℃ for at least 24 hours. After equilibration, fabric 2 was placed on fabric 1 with the fabric directions of the two fabrics aligned. Temperature measurements from the thermocouples in fabric 1 were collected for 1 minute, after which a single drop of the distilled water (1 ml) was applied by a micropipette (volume 1 ml), from a height which is close to but not contact with fabric (approximately 6 mm), onto the center of the concentric circles defined by the thermocouple points (measurement point 3 in Figure 3.3). During these tests, the environmental parameters consisted of an ambient temperature of 20 ± 1 ℃, relative humidity levels of 20 ± 2, 65 ± 2 or 80 ± 2%, and an air velocity of 0 to 0.2 m/s. Table 3.2 shows the testing conditions applied in this experiment. Three trials were performed at each combination of test conditions.

Table 3.2 Testing conditions of thermocouple-equipped fabric.

Fabric	Temperature (℃)	Relative humidity (%)	Volume of water (ml)
Cotton (C)	20±1	20±2	1
		65±2	
		80±2	
Polyester (P)	20±1	20±2	1
		65±2	
		80±2	

To further investigate the natural drying process of the two fabrics, a mass loss experiment was also performed. At an ambient condition of 20 ℃, 65%RH, using the same placement protocol as with the spot test, the two fabrics were placed on the

balance, with the readout set to zero. A 1ml drop of distilled water was then delivered from a height of approximately 6mm onto the center of concentric circles. In the process of natural drying, the resulting mass readings were recorded as the fabric dried. Three trials were carried out.

3.3 Results and discussions

3.3.1 Feasibility of thermocouples on fabric

Figures 3.6 and 3.7 present representative results for the ambient temperature measurements tested by thermocouple-equipped cotton and polyester fabrics, respectively. Traces 1 through 5 were recorded from the thermocouples placed into the fabrics, corresponding to the measurement points in Figure 3.3, while standards 1 and 2 refer to the two standard thermocouples described in section 3.2.2. During these validation trials, the temperature variations between the fabric thermocouple measurement points and the standard thermocouples were less than 0.2 ℃, which was within a reasonable experimental error and so indicated that the data from the fabric thermocouples can be considered accurate.

Over the forty minutes of data acquisition, the measured temperatures remained reasonably steady and the average temperatures of each point on cotton and polyester fabric were about 20.6±0.2 ℃ and 20.8±0.1 ℃, while the standard thermocouples recorded temperatures of approximately 20.8 and 20.9 ℃. The apparent difference in temperature between the two fabrics is mainly due to ambient temperature fluctuations. For each sensor, the temperature difference during the forty minutes is less than 0.1 ℃, satisfying the needs of tolerance of thermocouple in Japanese Industrial Standard (JIS) [26]. Moreover, the temperature differences of the thermocouples at the same moment are almost less than 0.5 ℃, meeting the needs of tolerance of thermocouple in JIS. Therefore, we concluded that these multipoint thermocouple-equipped fabrics can be served for thermometry of skin, garments and microclimates and other matrices.

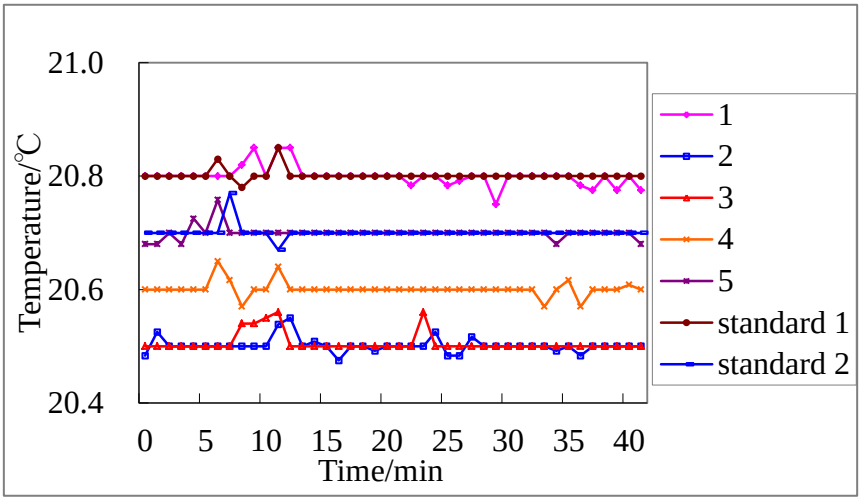

Figure 3.6 Ambient temperature measurements by cotton.

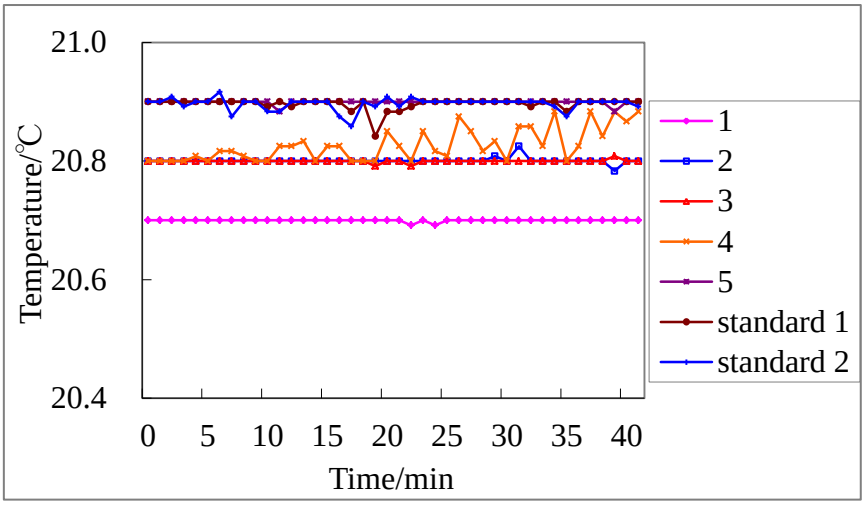

Figure 3.7 Ambient temperature measurements by polyester.

3.3.2 Temperature changes in wetted fabrics

Figures 3.8 and 3.9 show representative temperature changes in cotton and polyester fabric in the wetting and drying process at 20 ℃, 65% RH respectively. The horizontal axis represents time, and the vertical axis is the measured temperature.

In the case of cotton fabric, the temperature at the point where the water is dropped

immediately falls to approximately 16.5℃, a difference of about 4℃. The decrease at circumference (point 1 and 5) is just 1.5℃. For the polyester fabric, the temperature at the dropped point is almost the same with cotton fabric, although the decrease at circumference reaches to 3℃. Considering the areas over which the temperature declined, it can be deduced that at points 1 and 5 the water content of the cotton fabrics is less than that of the polyester. With the same volume of water, as hydroscopicity fiber, cotton fabric absorbs more water than the same mass of polyester fabric. Therefore, the diffusion area of polyester is wider than cotton fabric.

The points at different distances from the center of the circle show different temperature distributions. From 5 to 20minutes, after the application of the drop, the water moves outwards from the center of circle to the outer measurement points. During this process, the water transfer speeds of each point are different; the transfer to points 1 and 5 are the slowest. In the polyester fabric, it takes about 5 minutes for points 1 and 5 to register a temperature decrease, while points 2 and 4 only take about 1 minute. Considering the two figures, it is evident that there is a slight difference between the temperatures at the equidistant points 1 and 5, which is likely because even on the same fabric sample, the two points are not exactly on the same level, and this has an effect on the liquid moisture transfer.

Differences between temperature changes of the cotton and polyester fabrics are caused by the differences of diffusion rate of the water to the thickness direction, in-plane direction and the water absorbency of two materials.

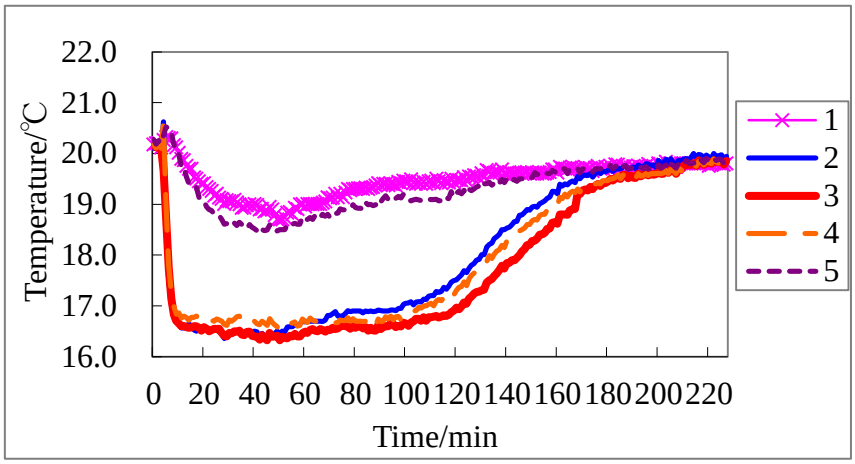

Figure 3.8 Temperature of wetted cotton fabric at 65% RH.

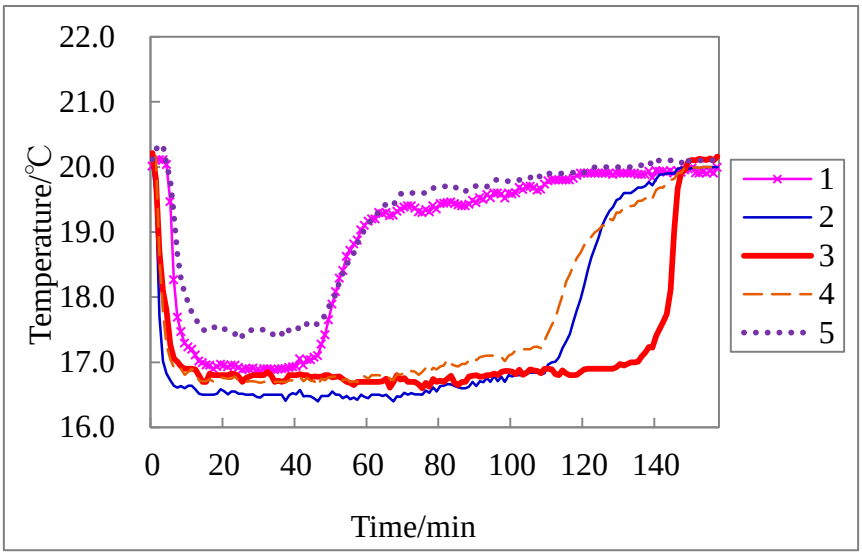

Figure 3.9 Temperature of wetted polyester fabric at 65% RH.

(1) Temperature changes of wetted fabrics at the dropped point

Figure 3.10 shows the temperature changes at the dropped point of wetted polyester and cotton fabric at different humidity levels.

During the moisture release of the two fabrics, the changes of surface temperature are primarily due to water evaporation, which lowers the surface temperature below

ambient.

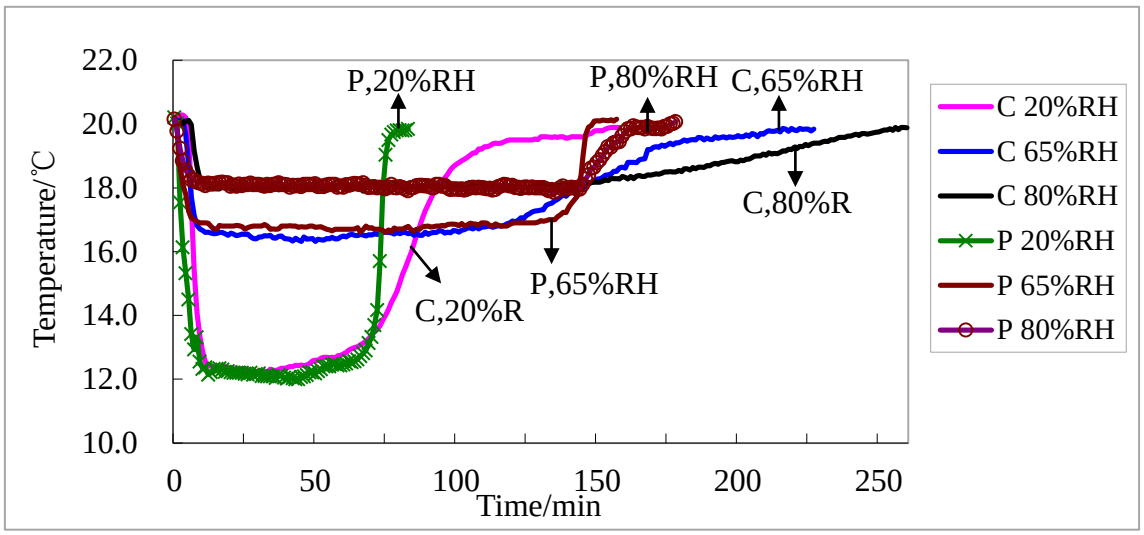

Figure 3.10 Temperature changes on the dropped point.

From Figure 3.10, it can be seen that the trend of surface temperature of dropped point is nearly the following stages: Immediately after water dropping, the temperatures increase slightly, then abruptly decreases, holds steady for a long time, and at last increase back to environmental temperature.

Initially, because the fabric absorbs water, and releases absorption heat simultaneously, there is slight increase in temperature. Subsequently, the local area at which the thermocouple is situated becomes essentially saturated with water vapor, and there is a gradient between this area and the surrounding ambient atmosphere that is at a much lower relative humidity. As the water evaporates and water vapor from the fabric surface diffuses into the surrounding air, the temperature at the measurement point declines.

However, the temperature of fabric will not decrease unlimitedly, when the dynamic heat balance is achieved, which means the heat loss by evaporation of water on

fabric equals to the heat gain by absorption from surroundings and the radiation and convection, the temperature of fabric will stabilize. The measured temperature can be considered the equivalent of the wet bulb temperature.

In the last stage, with the evaporation of liquid moisture, the moisture content of the dropped point decreases gradually, when the heat released by evaporation of moisture of fabric is less than the energy cumulated by fabric from absorption of vapor around the micro-climate and radiation, convection from surroundings, the surface temperature of fabric increases and reaches the equilibrium at this condition, which is the same with environmental temperature. The stage can be seemed as drying process of fabric.

In this experiment, the lowest temperature recorded during the dynamic heat balance were approximately 12.5, 16.7 and 18.0 ℃ at 20, 65 and 80% RH respectively, which are nearly the same as the wet bulb temperatures, which are 9.3, 15.8 and 17.7 ℃ respectively, especially at 80% RH. There is a slight difference in the lowest temperatures recorded between polyester and cotton, and this is likely because of differences in the rates of evaporation caused by the porosity of the fabrics, their yarn contents and other factors. The relative humidity of the micro-climate of dropped point of fabric can be calculated by:

$$R = \frac{e}{e_s(t)} \times 100, \tag{3.2}$$

where R is the relative humidity (%), e is the water vapor pressure, e_s is the saturated water vapor pressure. Both e and e_s can be calculated by the following [27, 28]:

$$e = e_s(t_w) - AP(t - t_w) \tag{3.3}$$

$$\log(e_s(T)/P) = 10.79586(1-T_0/T) - 5.02808\log(T/T_0) + 1.50474\times10^{-4}(1-10^{-8.29692(T/T_0-1)}) + 0.42873\times10^{-3}(10^{4.76955(1-T_0/T)}-1) - 2.2195983 \quad (3.4)$$

Here t is dry bulb temperature, 20℃; t_w is wet bulb temperature; P is the atmospheric pressure (101325Pa); A is 0.000662K^{-1}; T_0 is 273.16K.

From the equations (3.2) to (3.4), the relative humidity of the micro-climate at the adjacent dropped point of the three conditions of cotton and polyester fabric is listed in Table 3.3. At 20%RH, the relative humidity of polyester is 37.03%, which is about 20% higher than the humidity of environment. At 65%RH, it is about 6% higher; and at 80%, it is only about 2% greater. This is because, at higher humidity, the water vapor content in the air is so high that slows the evaporation of water on fabric surface, which leads to lower heat absorbed from fabric. As a result, the time required for the same fabric returning to room temperature is different at different humidity levels: with longer time periods required at higher ambient humidity levels.

Table 3.3 The relative humidity of micro-climate at the dropped point.

Fabric	20%RH		65%RH		80%RH	
	t_w (℃)	R (%)	t_w (℃)	R (%)	t_w (℃)	R (%)
C	12.7	41.86	16.3	68.88	17.9	81.69
P	12.0	37.03	16.6	71.03	17.9	81.69

Figure 3.10 also shows that the drying processes of the two fabrics are different, as can be deduced from the differing slopes of the temperature plots. At 65% RH, it takes about 10 minutes for polyester to return to room temperature, whereas the cotton fabric required approximately 1.5 hours. This is primarily because difference in the fabrics

result in dissimilar water transfer mechanisms. There are three ways of water transfer for hydroscopic fabric: absorb into the fiber, retain in pores and as free water between fibers and yarns [29]. As hydroscopic fiber, cotton absorbs water into the fiber as well as stores it in pores and as free water. However, as non-absorbent fiber, polyester fibers do not absorb water. During the drying process, it needs a little force for the free water and water retained in pores to release to the surroundings, but water absorbed by cotton fibers is difficult to release.

The results of mass loss measurements during the drying processes of the two fabrics are shown in Figure 3.11. In this figure, the horizontal axis is time and the vertical axis denotes the mass loss relative to the original mass. It is evident that polyester dries at a faster rate than cotton, which agrees with the earlier results in which the polyester fabric surface temperature returned to room temperature more quickly than the cotton.

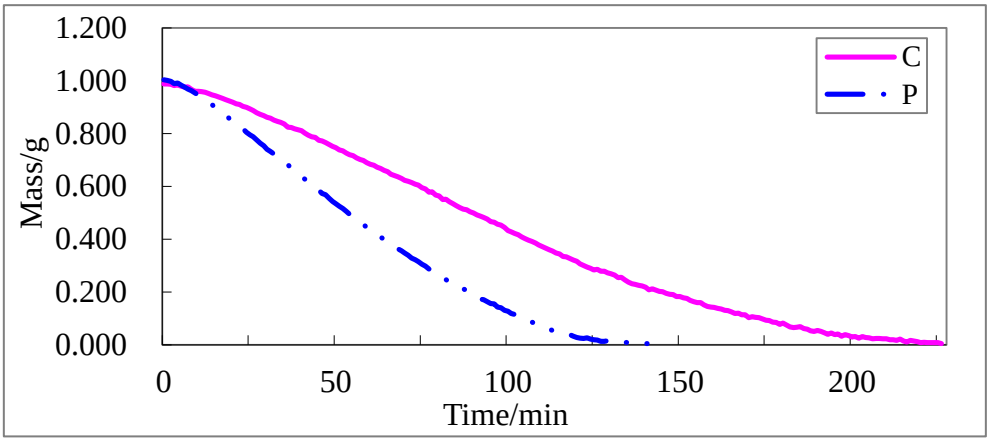

Figure 3.11 Mass loss during drying process at 65%RH.

Figure 3.12 shows the drying process of cotton and polyester fabrics expressed by changes of moisture mass and temperature at 65%RH. The horizontal axis represents

time, and the left-hand vertical axis denotes the liquid mass difference, the right-hand vertical axis is the temperature difference. The mass and temperature difference can be calculated by:

$$\Delta m_t = m_0 - m_t \tag{3.4}$$

$$\Delta T_t = T_0 - T_t \tag{3.5}$$

Here m_0 represents the liquid mass when t is 0 min. m_t is the liquid mass at the moment of time t. T_0 is the original temperature. T_t is temperature at the moment of time t.

In the case of the cotton fabric, at the moment of t_a (approximately 8min), the dropped point has achieved dynamic heat balance, even though the mass of liquid changed very little. Between times t_a and t_b, it maintains a constant drying rate, with an associated mass loss of about 0.7g. At the same time, the surface temperature of cotton fabric remains steady. From t_b to t_c, the temperature increases gradually and the mass loss drops, corresponding to the stage in which the drying rate decreases. After t_c, the changes of temperature and mass are minimal, and the fabric reaches to equilibrium with its surroundings. The polyester fabric also shows the same tendencies as the cotton, except that the time span between t_b and t_c is shorter because of the faster drying of polyester.

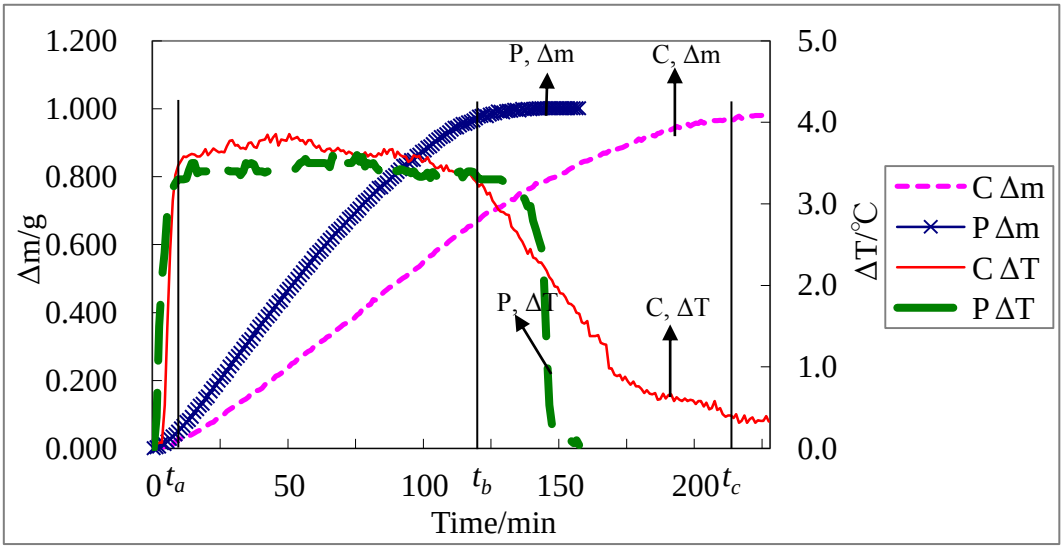

Figure 3.12 Temperature and mass change of the two fabrics.

(2) Temperature changes of wetted fabrics at circumference measurement points

Figures 3.13 and 3.14 show the temperature variations on both fabrics at measurement point 1 and 2, located on the circumference, which is 6 and 3 cm away from the center of the circle, at relative humidity of 20, 65 and 80%, respectively.

In Figure 3.14, however, where measurements at point 2 are presented, both cotton and polyester achieve approximately the same temperatures during the heat balance phase under the same humidity levels. Figure 3.15 presents more detailed plots highlighting the slight temperature increases caused by the heat release accompanying the initial water absorption. At lower RH levels, slightly higher temperatures are obtained. This phenomenon occurs because at lower relative humidity, the drop of water is absorbed to a greater extent upon its initial application to the fabric, thus producing greater heat of wetting, which in turn increases the fabric temperature.

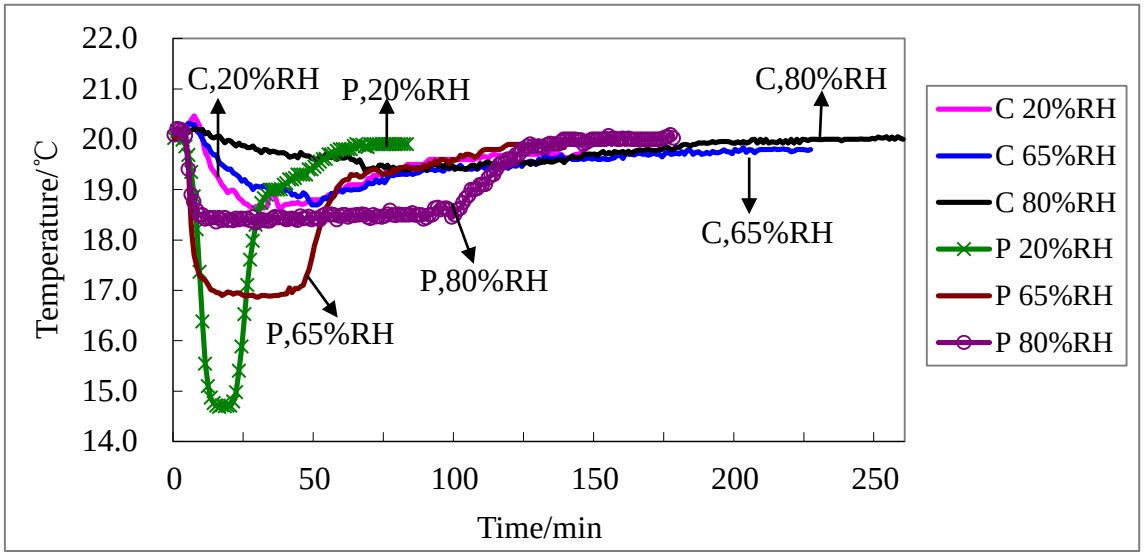

Figure 3.13 Temperature change with time of point 1.

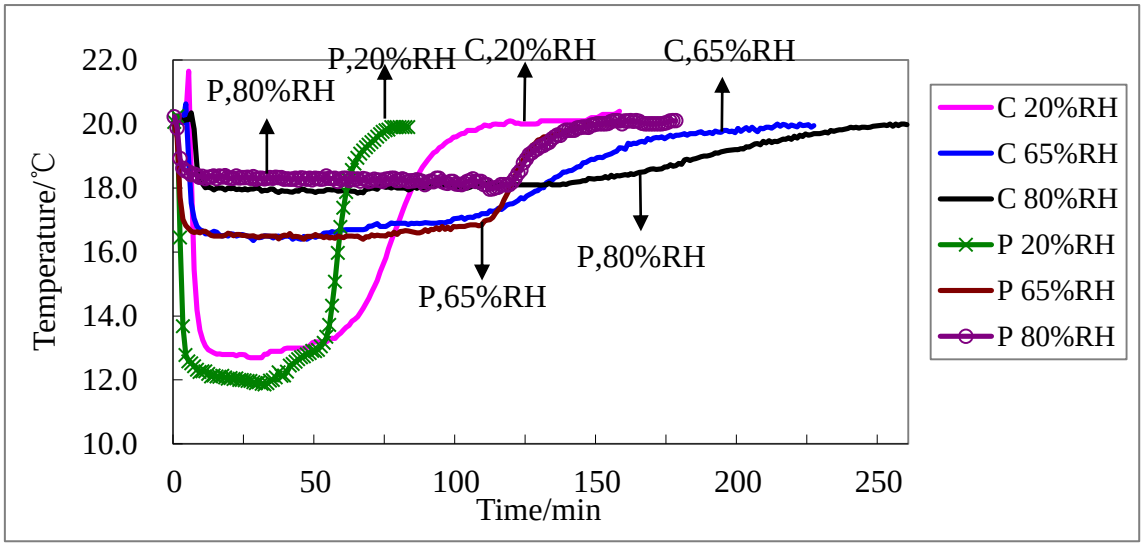

Figure 3.14 Temperature change with time of point 2.

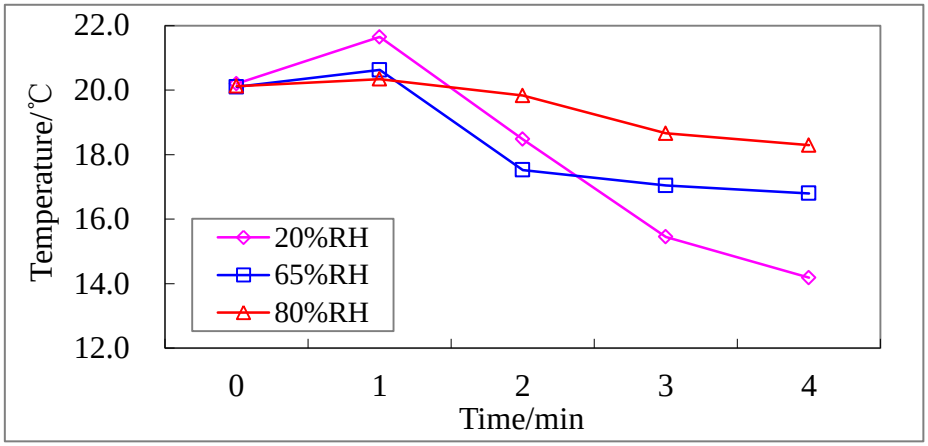

Figure 3.15 Initial temperature increases at point 2 on cotton fabric.

3.4 Development of thermocouple-equipped woven fabric

As thermocouple-equipped woven fabric, it should possess two functions: one is flexible then wearable, which is the basic function; the other is used as temperature sensor, which is an additional function. Therefore, in this study, a fabric with several pairs of thermocouples was woven with $2/40^{S}$ (14.5tex) polyester spun yarn as materials for fabric, ϕ0.1mm copper and ϕ0.1mm constantan as materials for thermocouple element wires. The arrangement is shown in Figure 3.16(a). A two-layer fabric was woven, and the thermocouple element wires were seemed as weft wadding threads in the middle between the top and bottom layer.

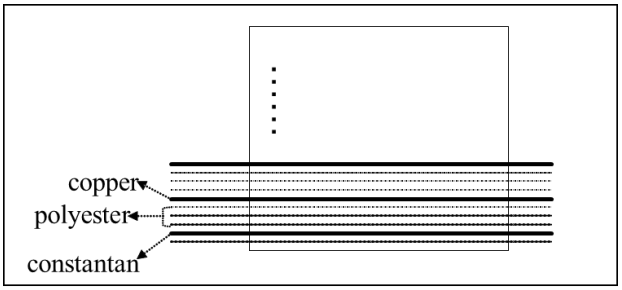

(a) Weft yarn arrangement in fabric.

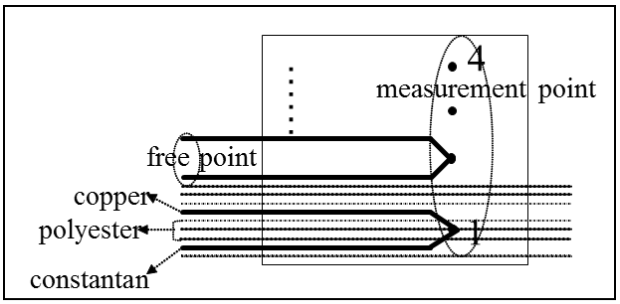

(b) Thermocouple in fabric.

Figure 3.16 Structure of textile thermocouple fabric.

In order to weave thermocouple fabric with copper and constantan welded together at only one point on the surface of fabric, and at the other point, the two kinds of metal fibers separated from each other, the fabric can be divided into three parts which are shown in Figure 3.17. Part I is to make sure two kinds of metal fibers separated from each other; Part II is used to interlace with face warp and back warp; Part III is used to make measurement points of thermocouple. The element wires are woven as weft floating.

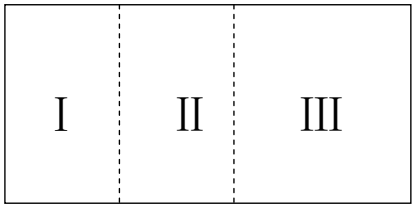

Figure 3.17 Three parts of fabric.

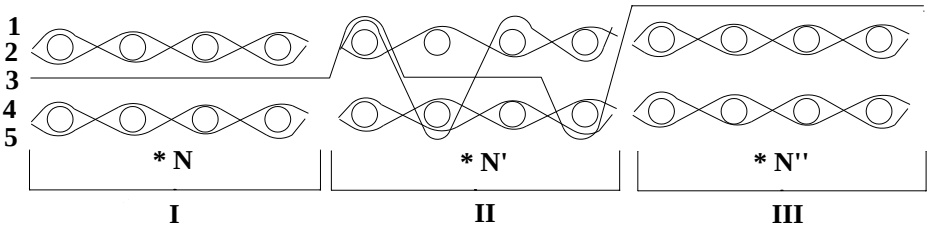

Figure 3.18 Weft cross section of fabric.

Figure 3.18 shows the weft cross section of the fabric in three different parts I, II and III, using polyester as weft 1, 2, 4, 5; polyester, copper and constantan as weft 3. In a repeat, the yarn arrangement number is polyester: copper: polyester: constantan as 3: 1: 3: 1, which is shown in Figure 3.18.

After weaving, the weft yarns of copper and constantan had been cut, and each group of mental fibers was welded to become a measurement point, which was

presented in Figure 3.16 (b). The real object of the thermocouple-equipped woven fabric is shown in Figure 3.19. The element wires are between two layers, with the junction on the fabric, which makes the fabric can not only measure temperature, but also can used for wearable clothes with little sense of discomfort.

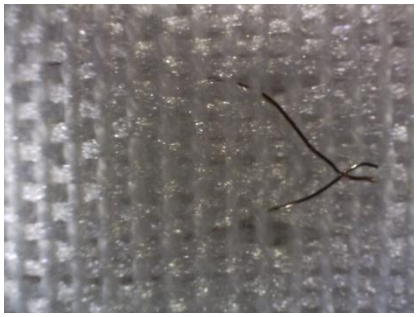

Figure 3.19 Real object of the thermocouple-equipped woven fabric.

3.5 Conclusion

In this study, the temperature variations during the wetting and drying process of cotton and polyester fabrics were measured by thermocouple sensors implanted in the fabrics.

The results provided useful information regarding temperature changes associated with the wetting and drying process. At the dropped point, the temperature was observed to fall down to approximately 12.5, 16.7 and 18.0℃ at 20, 65 and 80%RH respectively immediately, after which it remained stable for a relatively long time before finally returning to ambient temperature. At the circumference of the measurement circles, accompanied by liquid moisture diffusion, the associated drop in temperature was delayed and a constant temperature phase was again observed, followed by a return to ambient temperature that is achieved earlier than the dropped point. At 20℃, 65%RH, the lowest temperature of circumference points (6cm) on polyester fabric was essentially the same as the dropped point. With cotton fabric, however, these points were approximately 2.5 ℃ higher than the dropped point. This difference resulted from the hygroscopic nature of the cotton fabric, such that it absorbed more liquid water than the polyester, and hence its water diffusion area was not as wide and the resulting heat of evaporation was reduced. Essentially, following the application of a small amount of water, compared with polyester fabric, the cotton maintained a low temperature over a longer time period, about one and a half hours, within a narrow area. The recovery time for temperature of dropped point was longer with the increasing of the relative humidity. At 80%RH, the lowest temperature of dropped point was 17.9 ℃, which was essentially equal to the wet bulb temperature at this RH. With decreasing relative humidity from 80%

to 20%, the difference between the lowest temperature of fabric and the associated wet bulb temperature increased, with differences of 1 ℃ at 65%RH and 3 ℃ at 20%RH. This is most likely because the relative humidity of micro-climate of the dropped point was higher than environmental humidity. From the relationship between temperature change and liquid mass change on cotton and polyester, it showed the three stages of drying process, each with an associated temperature change. In addition, a slight temperature increases, about 2 ℃ was observed at the circumference point as soon as fabric was wetted, which was caused by heat of wetting.

Moreover, the woven method for a two-layer thermocouple-equipped fabric was shown in this study. The element wires are between two layers, with the junction on the fabric, which makes the fabric can not only measure temperature, but also can used for wearable clothes with little sense of discomfort.

Based on the investigation, it devised a method to analyze the performance of liquid water transfer on fabrics by measuring the associated temperature changes of fabric in the wetting and drying process following the application of water. With the help of thermocouples implanted in the fabric, both heat and moisture transfer process can be followed in real time. This technique simulates a three-dimensional, hollow fabric, in which temperature variations may be measured as a result of the distribution of temperature sensors in one of the layers. This method shows promise for the prediction of wearer discomfort levels resulting from the temperature decline associated with wetted fabrics.

References

[1] Parson K. Human thermal environments: The effects of hot, moderate and cold environments on human health, comfort and performance (Second edition). CVC Press, 2002. P. 156-195.

[2] Li Y, Plante AM, Holcombe BN. Fiber hygroscopicity and perceptions of dampness: Part II: Physical mechanisms. *Text. Res. J.* 1995; 65: 316-324.

[3] Plante AM, Holcombe BV, Stephens LG. Fiber hygroscopicity and perceptions of dampness: Part I: Subjective trials. *Text. Res. J.* 1995; 65: 293-298.

[4] Yasuda T, Miyama M. Dynamic water vapor and heat transport through layered fabrics. *Text. Res. J.* 1992; 62: 227-235.

[5] Le CV, Tester DH, Buckenham P. Heat and moisture transfer in textile assemblies: Part II: Steaming of blended and interleaved fabric-wrapper assemblies. *Text. Res. J.* 1995; 65: 265-272.

[6] Wang Z, Li Y, Zhu YQ, Luo ZX. Radiation and conduction heat transfer coupled with liquid water transfer, moisture sorption, and condensation in porous polymer materials. *J Appl. Polym. Sci.* 2003; 89: 2780-2790.

[7] Zhou LY, Feng XW, Du YF, Li Y. Characterization of liquid moisture transport performance of wool knitted fabrics. *Text. Res. J.* 2007; 77: 951-956.

[8] Guo YP, Li Y, Yao L, Liu R, Cao XY, Cao ML. Skin Temperature, Stratum corneum water content and transepidermal water loss distributions during running. *J Fiber Bioeng Inform.* 2011; 4(3): 253-266.

[9] Song WF, Liu Q, Yu WD. Investigation on effective heat conductivity of fibrous assemblies by fractal method. *J Fiber Bioeng Inform.* 2011; 4(1): 59-69.

[10] Hu DH, Cheng JX, Zhou XH. A model of heat and moisture transfer through parallel pore textiles. *J Fiber Bioeng Inform.* 2011; 3(4): 250-255.

[11] Li Y, Zhu QY, Yeung KW. Influence of thickness and porosity on coupled heat and liquid moisture transfer in porous textiles. *Text. Res. J.* 2002; 72: 435-446.

[12] Jiang XY, Zhou XH, Weng M, Zheng JJ, Jiang YX. Image processing techniques and its application in water transport through fabrics. *J Fiber Bioeng Inform.* 2010; 3(2): 88-93.

[13] Wang FM, Kalev K, Gao CS, Ingvar H, George H. Development and validation of an empirical equation to predict wet fabric skin surface temperature of thermal manikins. *J Fiber Bioeng Inform.* 2010; 3(1): 9-15.

[14] Zhu QY, Yang J, Xie MH. Effects of zeta potential and fiber diameter on coupled heat and liquid moisture transfer in porous polymer materials. *J Fiber Bioeng Inform.* 2010; 3(1): 16-21.

[15] Mao AH, Li Y, Luo XN, Wang RM. Development of computational algorithms for clothing thermal functional simulation. *J Fiber Bioeng Inform.* 2010; 2(4): 259-266.

[16] Alber-Wallerstrom B., Holmer I.. Efficiency of sweat evaporation in unacclimatized man working in a hot humid environment. *Eur J Appl Physiol.* 1985; 54: 480-487.

[17] Holcombe BV, Hoschke BN. Dry heat transfer characteristics of underwear fabrics. *Text. Res. J.* 1983; 53(6): 368-374.

[18] Watkins DA, Slater K. The moisture-vapour permeability of textile fabrics. *J. Text. Inst.* 1981; 72(1): 11-18.

[19] Takako F, George H. Differences in comfort perception in relation to local and whole body skin wittedness. *Eur. J. Appl. Physiol.* 2009; 106: 15-24.

[20] Hu JY, Li Y, Yeung KW, Wong ASW, Xu WL. Moisture management tester: A method to characterize fabric liquid moisture management properties. *Text. Res. J.* 2005; 75(1):57-62.

[21] Yao BG, Li Y, Hu JY, Kwok YL, Yeung KW. An improved test method for characterizing the dynamic liquid moisture transfer in porous polymeric materials. *Polym Test.* 2006; 25:677-689.

[22] Lyons DW, Vollers CT. The drying of Fibrous Materials. *Text. Res. J.* 1971; 41: 661-668.

[23] Ziegler S, Frydrysiak M. Initial research into the structure and working conditions of textile thermocouples. *Fibres Text. East Eur.* 2009; 17: 84-88.

[24] Zhu CH, Takatera M. Weaving and performance study on wearable textile thermocouple fabric. International Congress on Innovative Textiles (ICONTEX). Istanbul, Turkey, 2011.

[25] Harnett PR, Mehta PN. A survey and comparison of laboratory test methods for measuring wicking. *Text. Res. J.* 1984; 54(7): 471-478.

[26] Japanese Standards Association (1995): JIS C1602-1995.

[27] Japanese Standards Association (1995): JIS Z8806-1995.

[28] Nantou Y. “Sensa to kiso gijutsu”, Kougaku Tosho Kabushiki Kaisha. Tokyo: 1994. P. 72, In Japanese.

[29] Schneider AM, Hoschke BN. Heat transfer through moist fabrics. *Text. Res. J.* 1992; 62: 63-66.

Chapter 4

A new thermocouple technique for the precise measurement of in-plane capillary water flow within fabrics

Chapter 4 A new thermocouple technique for the precise measurement of in-plane capillary water flow within fabrics

4.1 Introduction

The transport of liquids through textiles plays an important role in their applications. In general, wetting is the displacement of a solid-air interface by a solid-liquid interface. The motion of a liquid through a fibrous assembly, such as yarn or fabric, may be driven by external forces or solely by capillary action. The spontaneous transport of a liquid driven into a porous system by capillary forces is termed “wicking”. Because capillary forces are caused by wetting, wicking is essentially the outcome of spontaneous wetting in a capillary system [1-3]. Wicking takes place only in wet fabrics or when fabrics come into contact with water, and the contact angle determines their wicking behaviour. A lower contact angle results in higher wicking coefficients [4].

Wicking in fabrics has been widely researched both in academia and industry because it plays an important role in many textile applications, including the design and use of sports wears and industrial uniforms, as well as in various processes such as dyeing, finishing and filtration. In applications such as active sportswear, exercise garments, work clothing, intimate apparel, and footwear, the concept of moisture management is utilized to prevent or minimize the collection of liquids on the skin of the wearer due to perspiration. This is done by quickly wicking of diffusing the liquid

through a hydrophobic fiber inner layer to an outer hydrophilic layer and then evaporated it to the atmosphere [5].

A variety of techniques are used to experimentally study wicking in fabrics, the simplest of which consists of following the movement of liquid throughout the textile structure by using colored water, camera or image analysis techniques and so on [2, 3, 6-15]. This can be performed when the fabric is perpendicular to, and partly immersed, in a liquid bath or when a drop of liquid is applied to a fabric or yarn and subsequently spreads. The Byreck method, or DIN 53924 [11, 15, 16] is a conventional method of assessing the water absorbency of fabrics. This method is to use a preconditioned strip of the test fabric, suspended vertically with its lower end immersed in a reservoir of distilled water, to which may be added a dye (of a type known not to affect the wicking behavior) for tracking the movement of water. After a fixed time has elapsed, the height reached by the water in the fabric above the water level in the reservoir is measured. However, when applying this method, it is important to take into consideration the influence of the dye applied to color the liquid on the absorption properties of the fabric, as well as variances in the apparent liquid flow front caused by different observational positions and the effects of gravity [17]. Although present-day photographic and image analysis technologies can easily track the surface capillary flow within a fabric, these technologies are not always suitable in the case of multilayers, thick fabrics or composite materials. An alternate technique is to weigh the fabric or yarn during capillary wicking [18, 19]. However, this method is too sensitive to use with yarns, since in these textiles the wetting force exceeds the effects of capillary forces [2, 9], and it will not show the effect of capillary exactly. Yet another approach consists of measuring the wicking length by applying liquid-sensitive sensors, which track

electrical capacitance, humidity and other factors, at regular intervals along the fabric [17, 20, 21]. This approach also has some associated challenges: the sensors are expensive, and are not suitable for testing fabrics while they are being worn, and may have limited durability.

In the work reported herein, a new method of experimentally measuring capillary liquid flow by using thermocouple array was developed, based on previous studies of temperature variations in fabrics during the wetting and drying processes [22]. As each thermocouple is physically very small and measures temperature over a correspondingly small area, thermocouple array have numerous potential applications, not only in studying liquid water transport but also in following textile water content in real-time. By employing removable, flexible thermocouples, this method can be used to determine the wicking length of liquid moving through fabrics over time without the requirement to add dyes to the liquid. It is also adaptable to many different textile structures, including woven and nonwoven fabrics, as well as yarns. Moreover, this method can be applied to thick fabrics simply by modifying the thermocouple measurement points. The aim of this work was therefore to design and test a new experimental technique for measuring capillary liquid flow, and to investigate the viability of applying this method to estimate the water contents of fabrics.

4.2 Basic theory for the in-plane capillary liquid flow

The basic theory of wicking in textiles is introduced in Chapter 2. Figure 4.1 shows the in-plane capillary liquid flow. For the distance *h* in Equation (2.5), as shown in Figure 4.2, is the distance between water level in the fluid reservoir and fabric laid horizontally (the first measurement point). As *h* is very slight, in order to simplify the calculation, the horizontal wicking distance of the water is therefore given as Equation (2.6).

$$L = \left(\frac{R\gamma \cos\theta}{2\eta} \right)^{1/2} t^{1/2} \tag{2.6}$$

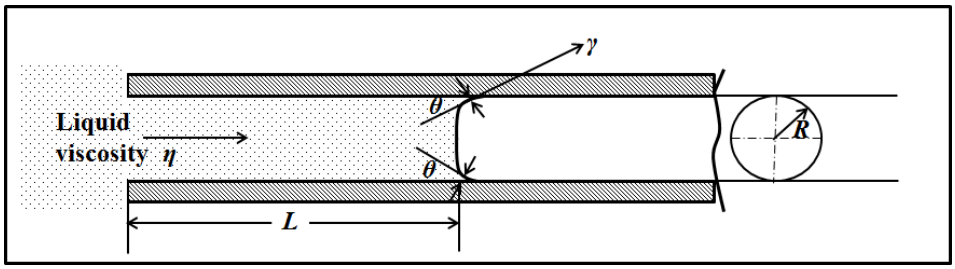

Figure 4.1 Capillary action for in-plane capillary liquid flow.

4.3 Experimental

The experimental trials were divided into two parts. The initial trials verified the applicability of the new experimental technique of using thermocouple array to measure capillary liquid flow, while subsequent work investigated the feasibility of employing this method to estimate the equilibrium water contents of wetted fabrics.

4.3.1 Experimental for measuring capillary liquid flow

(1) Test apparatus

Figure 4.2 presents diagrams of the test apparatus used to measure capillary liquid flow through the fabrics. The apparatus consisted of an array of nine thermocouple measurement points set 10 mm apart and sitting on foam polystyrene for heat insulation. The thermocouples were T-type, made from copper and constantan element wires of 0.1 mm in diameter [22]. The standard temperature range is from -200 ℃ to 350 ℃, and the accuracy of the thermocouple is within 0.5 ℃. The temperature data were collected and recorded in a sampling rate of $5s^{-1}$, or 5 data points per second automatically.

For the woven fabric, the wetted end of the fabric strip was clipped to a weight that produced a tension of 5.0gf/cm [17]. This functioned both to keep the fabric end immersed in the 20 ± 1 ℃ ion-exchanged water and to ensure the rest of the fabric strip remained in contact with the sensor array. The absolute minimum amount of tension necessary was applied, since excess tension can strain the fabric and alter its wicking performance. For the knit fabric, because it is stretchy, a slight tension may cause the stretch of fabric, the tension for it was only its own weight. The other end of the fabric was fixed so as to keep it taut throughout the experimental trial. The water level in the

fluid reservoir was maintained at a constant height by perforating a hole on the reservoir to keep the water level the same before each experimental trial and suppressing water evaporation during the experiment. As the fabric absorbed water, changes in temperature were measured by the thermocouple array.

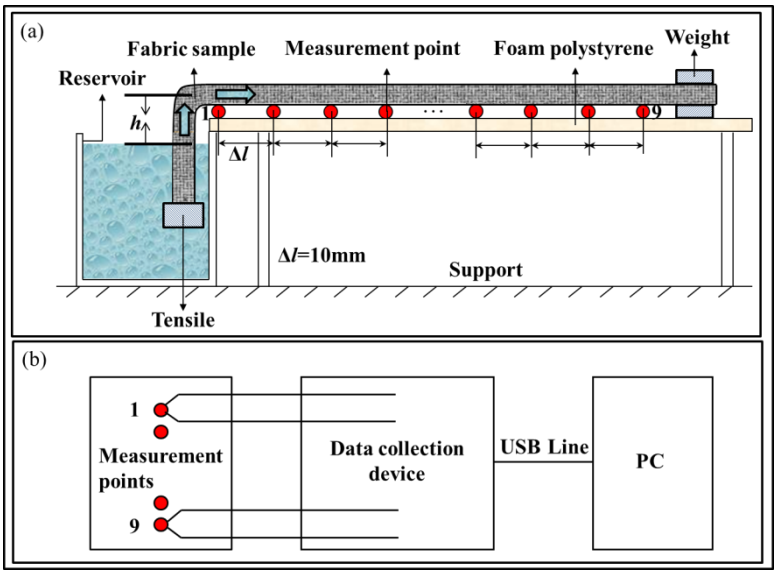

Figure 4.2 Thermocouple test apparatus: (a) Schematic diagram of thermocouple method; (b) Block diagram of the overall system.

(2) Principle of the measurement

The temperature of the fabric at the liquid flow front will change during the process of water absorption because of heat transference associated with both wetting and evaporation. As the fabric initially absorbs water, wetting heat is generated and the local temperature temporarily increases, after which it begins to drop [22]. These temperature variations are measured by the thermocouple at each measurement point and are relayed to and recorded by a computer.

Figure 4.3 shows the relationship between temperature and time during the liquid

flow process of a cotton/polyester fabric. Because of absorption heat, the fabric temperature increases, and then it goes down for the reason of evaporation larger than absorption till it reaches about the wet bulb temperature [22].

Since the fabric temperature will rise because of the absorption of liquid, if the temperature T at time t increases 0.5 ℃ in less than 10 seconds, then t is defined as the arrival time, as shown in Figure 4.3. The 10 second time scale was determined on the basis of measurement error and the stability of measured temperature. If the temperature at time t increases 0.5 ℃ at $t_{T+0.5}$ in which the interval is more than 10 seconds, then the arrival time is defined as Equation (4.1). However, if the wetting heat is minimal compared with heat loss via evaporation, then the temperature at the flow front will decrease. In this case, the arrival time of the flow front is defined as the time at which the temperature is 0.5 ℃ greater than the temperature at time t+10 (s), as shown in Equation (4.2).

$$t_n = t_{T+0.5-\mathrm{C}} - 10\mathrm{s} \tag{4.1}$$

$$t_n = t_{T-0.5-\mathrm{C}} - 10\mathrm{s} \tag{4.2}$$

Here T (℃) is the temperature at the arrival time t (s). As nine measurement points are set in this experiment, n refers to 1 to 9.

As shown in Figure 4.3, the time required for liquid flow between any two measurement points n and n+1 can be calculated according to Equation (4.3).

$$\Delta t_{n\to n+1} = t_{n+1} - t_n,\ n=1, 2,\ldots 8. \tag{4.3}$$

The overall time ($Time_n$) from the zero of the flow time to the point n+1 can be calculated according to Equation (4.4).

$$Time_n = \Delta t_{1\to 2} + \Delta t_{2\to 3} + \cdots + \Delta t_{n\to n+1} \tag{4.4}$$

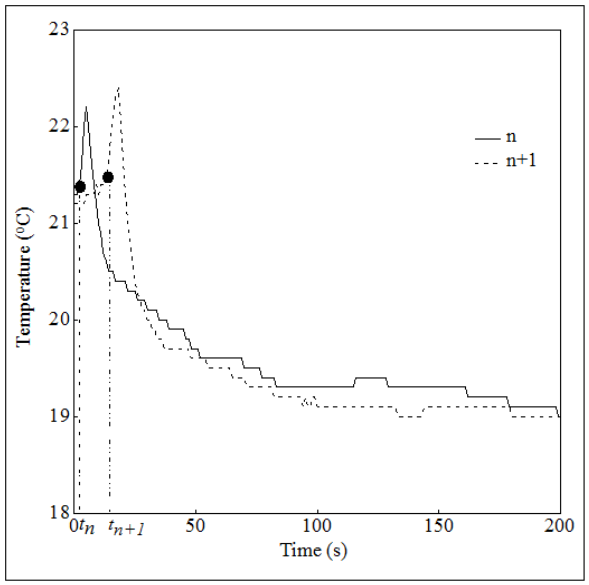

Figure 4.3 Temperature variations over time in a cotton/polyester fabric.

(3) Test samples

Three kinds of plain woven fabrics and two kinds of knitted fabrics were used in this work, with the specifications shown in Table 4.1.

Prior to testing, fabric samples were washed with soap for 35 minutes, then rinsed with water for 50 minutes to prevent soap remaining on the fabric samples, and dried by air at constant environmental condition of 20 ± 1 ℃ and a constant relative humidity (RH) of 65 ± 2%. Then test specimens (25 by 3 cm) were carefully cut from each fabric at varying locations along the warp, weft and 45 ° bias directions. Experiments were performed at a constant temperature of 20 ± 1 ℃ and a constant relative humidity (RH) of 65 ± 2%. Five samples for each direction of each fabric were tested, and the averages and standard deviations were determined. A diagram of a typical fabric strip sample as used in these trials is presented in Figure 4.4. The portion of the fabric that is bent

towards the water reservoir is 5 cm long, and 4.7 or 4.8 cm length of it is immersed in the ion-exchanged water, while the horizontal section is 9 cm and is marked at 1 cm intervals.

Table 4.1 Specifications of test samples.

Sample name		C	C/P-1	C/P-2	C-k	P-k
Fiber content		100% Cotton	35% Cotton 65% Polyester	35% Cotton 65% Polyester	100% Cotton	100% Polyester
Fabric type		Woven	Woven	Woven	Weft knit	Weft knit
Yarn count (tex)	Warp	28.0	12.5	13.5	24	21
	Weft	28.0	14.5	13.5		
Fabric density (cm^{-1})	Warp/Wale	27	56	56	27	32.5
	Weft/Course	22	28	28	18.5	22
Mass per unit area (g/m^2)		153.52	114.60	111.02	176	165
Thickness (mm)		0.745	0.442	0.569	1.02	1.03
Porosity [2]		86.62	82.53	86.41	88.80	88.39

To assess the validity of our new measurement technique, we simultaneously applied the horizontal Byreck method [24] to measure liquid flow through the same fabrics. In the following discussions, we refer to this protocol as the Byreck method and the new technique simply as the thermocouple method.

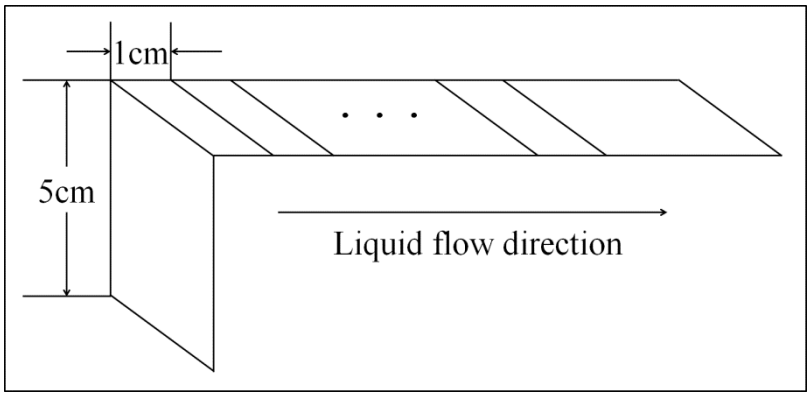

Figure 4.4 Diagram of a typical fabric sample as used in water flow trials.

4.3.2 Predicting water content based on temperature differences in fabrics

Initially, experimental trials were carried out with the aim of investigating the relationship between fabric temperature and water content, using square sections of fabric. Moreover, the relationship between water content and difference of fabric and room temperatures were obtained, which are used for estimating water content from the temperature difference.

Prior to each trial, test specimens were wetted by soaking in distilled water for 24 hours and squeezed to make sure no water dripped from the fabric. Then lay the fabrics on the foam polystyrene placed on the balance, which was set zero at the beginning of the experiment. The mass and temperature of each wetted specimen were measured and recorded during the subsequent drying process. The continuous mass was measured and recorded by the GF-600 balance (A&D Company, Limited), with the resolution of 0.001g. The temperature was measured and recorded by three thermocouples with the measurement points set between two fabrics.

We next carried out experimental trials designed to investigate the relationship

between temperature and water content at different locations along the fabrics when water flow had reached equilibrium.

Measurements of the equilibrium wicking lengths were performed using the same apparatus as shown in Figure 4.2, applying thermocouple measurement points as summarized in Figure 4.5. The first measurement point was located immediately adjacent to the water reservoir, followed by additional ten measurement points every 3 cm and then eleven measurement points at 1 cm intervals. Fabric specimens 55 cm in length and 3 cm wide were used and the equilibrium wicking length was determined by dipping a 4.5 cm end portion of the sample in a water reservoir for 12 hours [23]. Temperatures along the fabric at the thermocouple measurement points were recorded during this time period, and the temperature of each measurement point was assumed to be the average temperature of the segment to which the measurement point was attached. The temperature difference of the fabric at each segment was calculated by subtracting the measured temperature at each measurement point from room temperature.

When the 12 hours wicking time had elapsed, every 1 cm segment of the fabric centred on each of the thermocouple measurement points was cut off and weighed to calculate the water content. The water content of each section of fabric (M) was calculated using Equation (4.5).

$$M = \frac{W_1 - W_2}{W_2} \times 100\% . \tag{4.5}$$

Here, W_1 is the mass of the wet fabric segment immediately after being removed from the test specimen, and W_2 is the mass of the same fabric segment after drying.

A 100% cotton fabric (C) was used in these experiments and six trials were performed along the weft direction at a constant temperature of 20 ± 1 ℃ and 65 ± 2% RH.

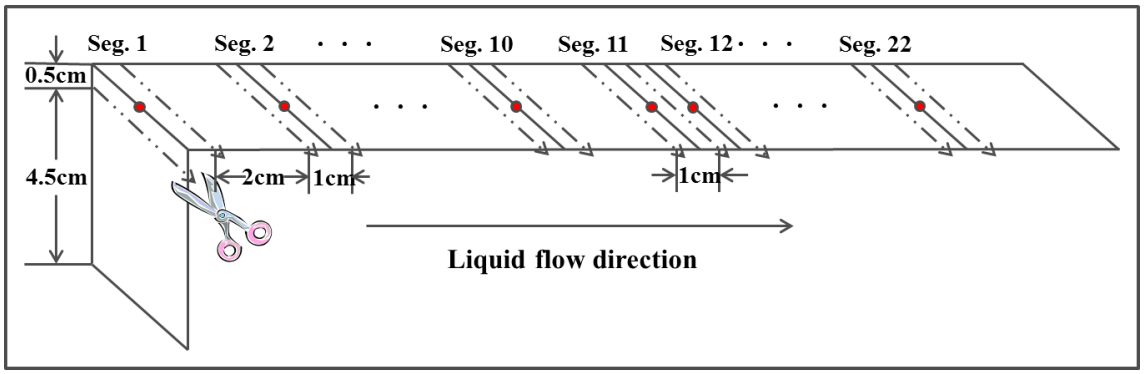

Figure 4.5 A typical fabric strip sample as used in equilibrium water flow trials, showing thermocouple locations.

4.4 Results and discussion

4.4.1 The feasibility of the thermocouple method

Figure 4.6(a) summarizes the results of measurements of wicking length over time during wetting of cotton fabric in the warp direction, as measured by both the thermocouple array and the Byreck method. Figure 4.6(b) plots the same results but against the square root of time, which Equation (2.6) suggests should produce a straight line.

It is evident that both methods generated data showing essentially the same trends: as wetting time increases, so does wicking length. Equation (2.6) predicts that the wicking length will be zero at time zero, although, as shown in Figure 4.2, there is a finite distance between the water surface and the nearest measurement point, and so these plots do not go through the origin. Figure 4.6(b) shows that the plots of wicking length versus square root of time are highly linear, with coefficients of determination above 0.99, in agreement with Equation (2.6). The wicking coefficient of the cotton fabric can be obtained from these data, and values of 0.3099 and 0.3084 are calculated from the thermocouple and Byreck method data, respectively. There is evidently a slight difference between the two methods such that, at the same wicking length, the time measured by the thermocouple method is slightly shorter than that determined by the Byreck method. This is mainly because the Byreck method requires that the water front be determined by visual analysis of color change, and so there is an associated time lag between the actual and the observed water front. The thermocouple method, being automated, with a high frequency of data collection, is therefore more precise than the Byreck method. Figure 4.7 and Figure 4.8 show the results for cotton fabric (C) in the

weft and bias direction, respectively.

Liquid flow throughout the other fabrics (C/P-1, C/P-2 and C-k) was also measured by both the thermocouple array and Byreck techniques. The results were shown from Figure 4.9 to Figure 4.17 and very similar results were obtained. Because of the hydrophobicity of polyester knit fabric (P-k), the wicking length is almost zero which cannot be measured and recorded by both techniques. Therefore, the results of polyester fabric cannot be shown.

Table 4.2 lists the wicking coefficients determined for fabric samples in the warp, weft and 45º bias directions, as meas ured by the thermocouple and Byreck methods. The relative differences between the results determined by the two methods ΔW are also provided, as calculated according to Equation (4.6).

$$\Delta W = \left| \frac{W_T - W_B}{W_B} \right| \times 100\% . \tag{4.6}$$

Here, W_T is the wicking coefficient determined by the thermocouple method and W_B is the wicking coefficient resulting from the Byreck method. As the ΔW values in Table 4.2 demonstrate, the differences between both methods are small.

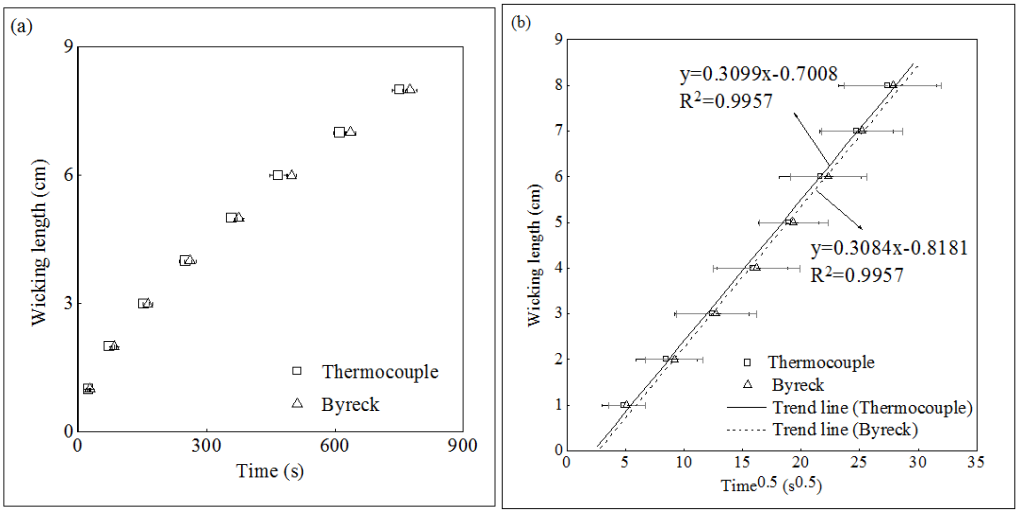

Figure 4.6 Comparison of the results of thermocouple and Byreck measurements for cotton fabric in the warp direction: (a) Relationship between the wicking length and time; (b) Relationship between wicking length and square root of time.

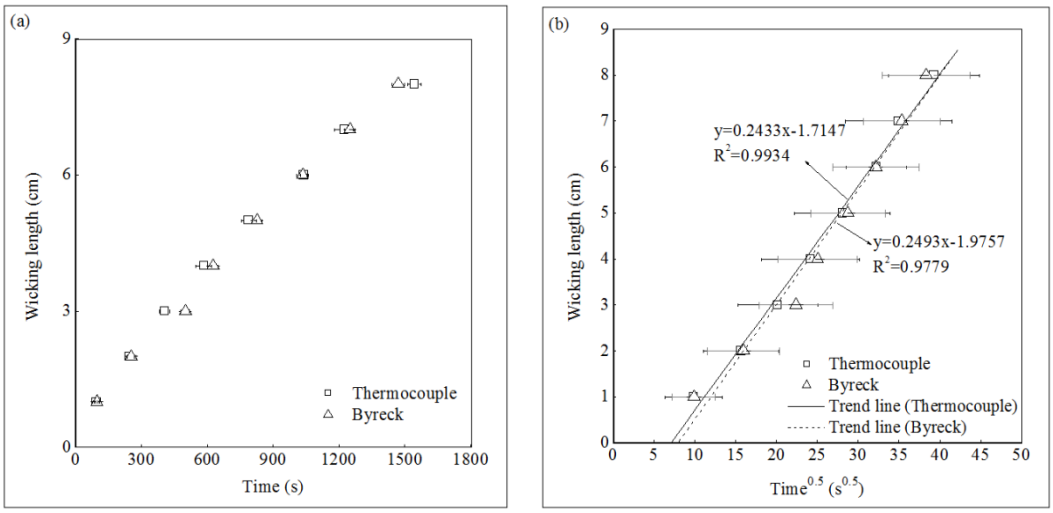

Figure 4.7 Comparison of the results of the two measurements for cotton fabric in the weft direction: (a) Relationship between the wicking length and time; (b) Relationship between wicking length and square root of time.

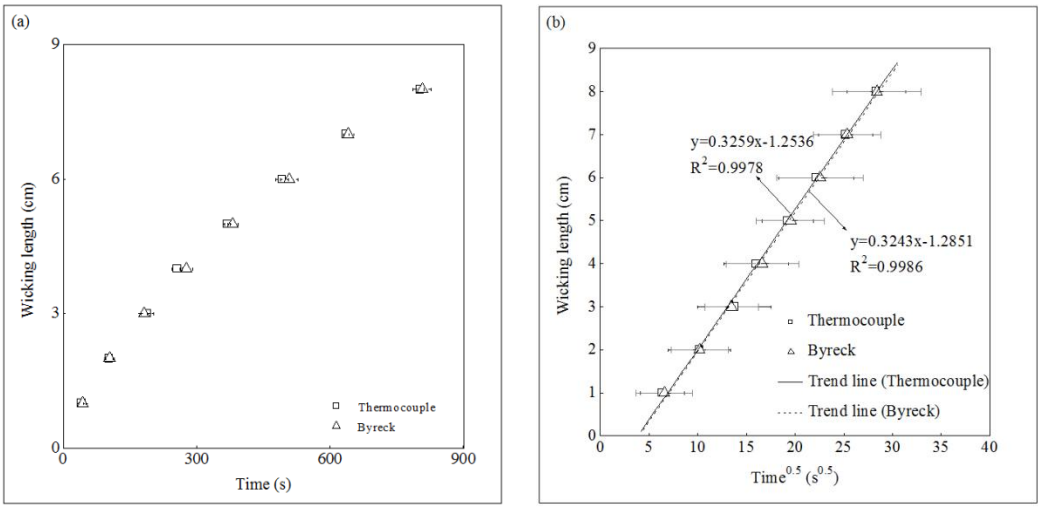

Figure 4.8 Comparison of the results of the two measurements for cotton fabric in the 45° bias direction: (a) Relationship between the wicking length and time; (b) Relationship between wicking length and square root of time.

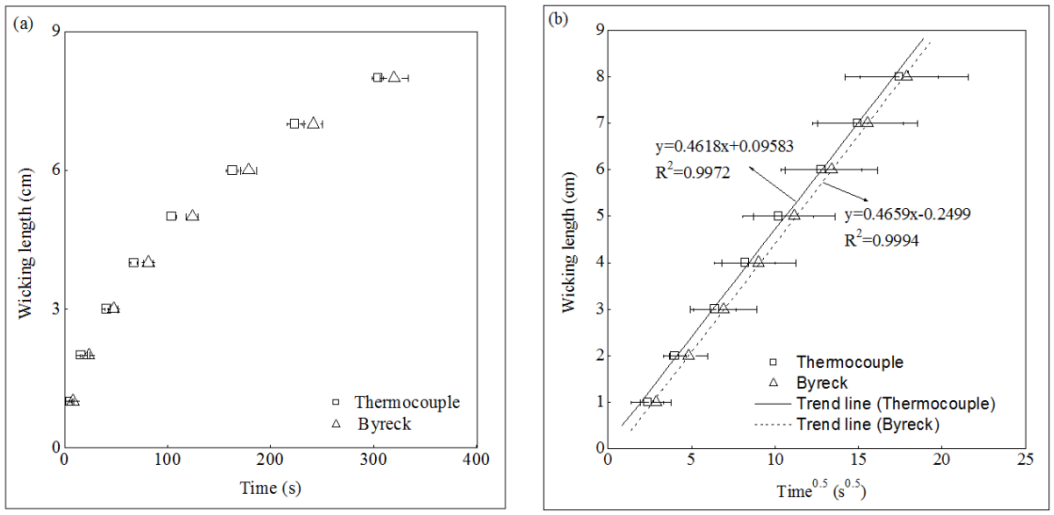

Figure 4.9 Comparison of the results of the two measurements for cotton/polyester fabric (C/P-1) in the warp direction: (a) Relationship between the wicking length and time; (b) Relationship between wicking length and square root of time.

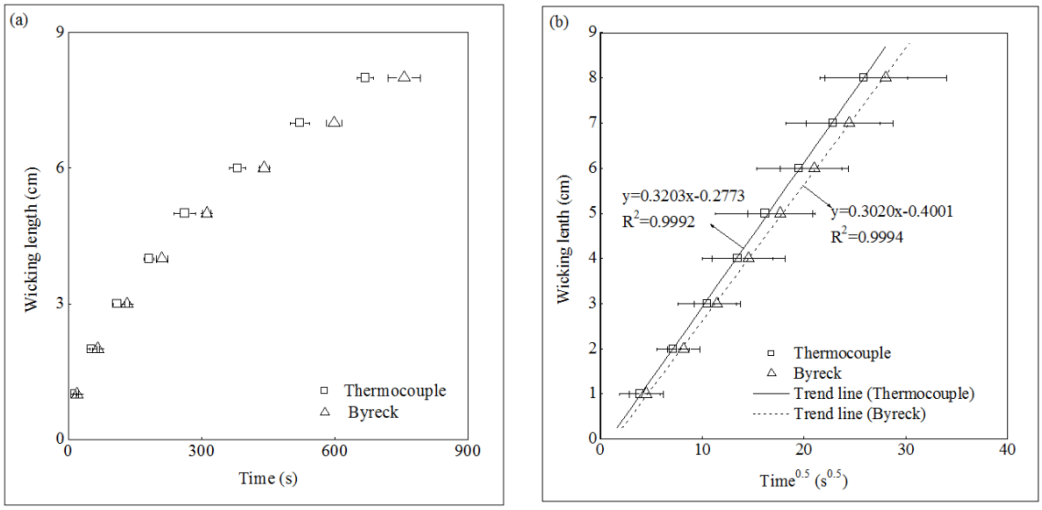

Figure 4.10 Comparison of the results of the two measurements for cotton/polyester fabric (C/P-1) in the weft direction: (a) Relationship between the wicking length and time; (b) Relationship between wicking length and square root of time.

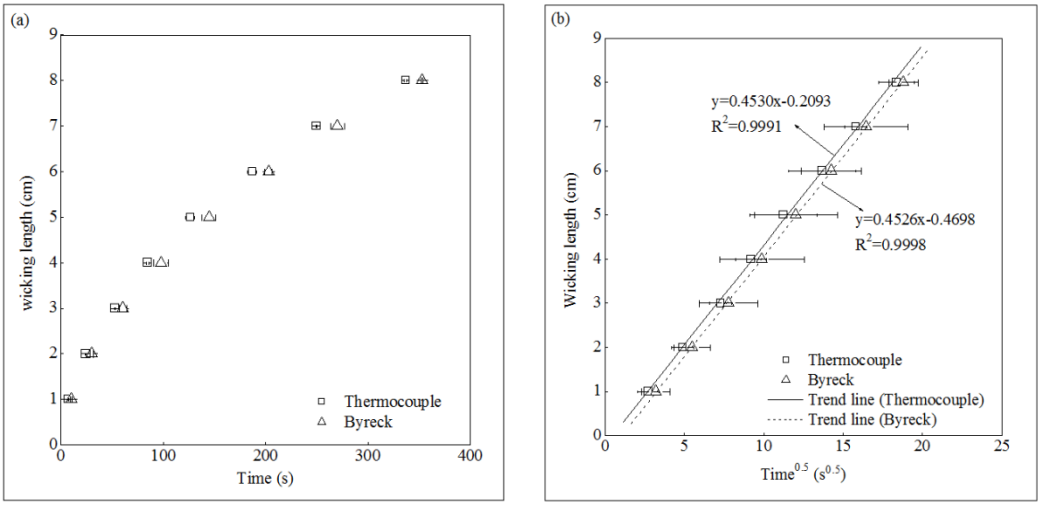

Figure 4.11 Comparison of the results of the two measurements for cotton/polyester fabric (C/P-1) in the bias direction: (a) Relationship between the wicking length and time; (b) Relationship between wicking length and square root of time.

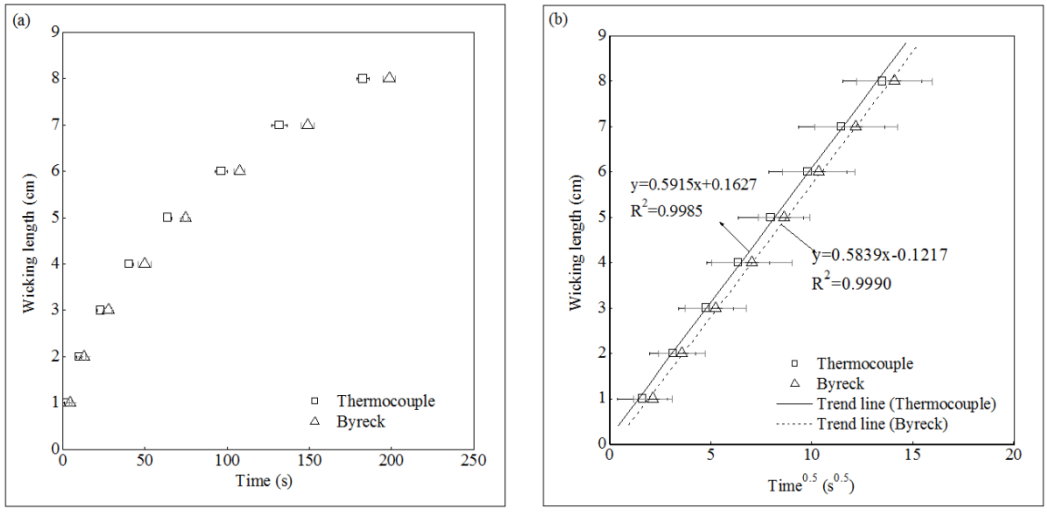

Figure 4.12 Comparison of the results of the two measurements for cotton/polyester fabric (C/P-2) in the warp direction: (a) Relationship between the wicking length and time; (b) Relationship between wicking length and square root of time.

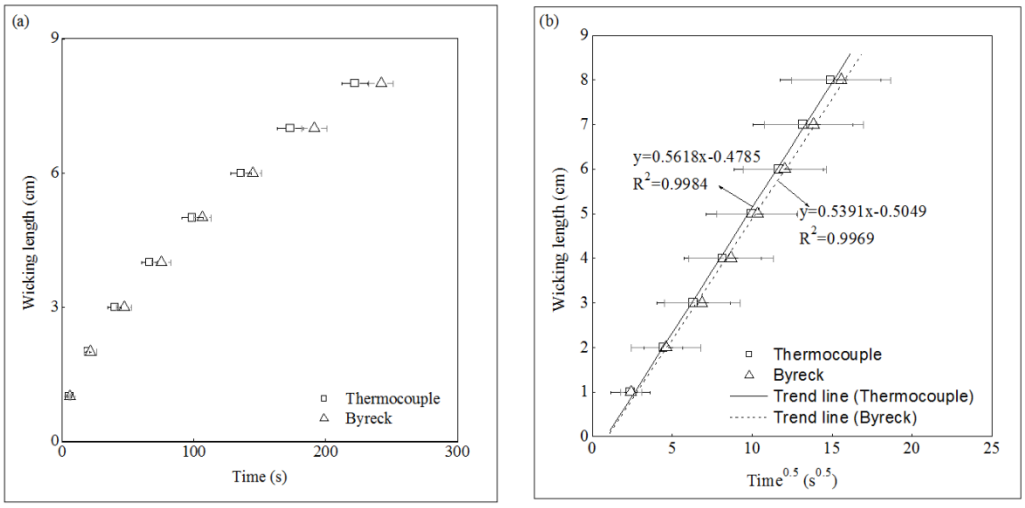

Figure 4.13 Comparison of the results of the two measurements for cotton/polyester fabric (C/P-2) in the weft direction: (a) Relationship between the wicking length and time; (b) Relationship between wicking length and square root of time.

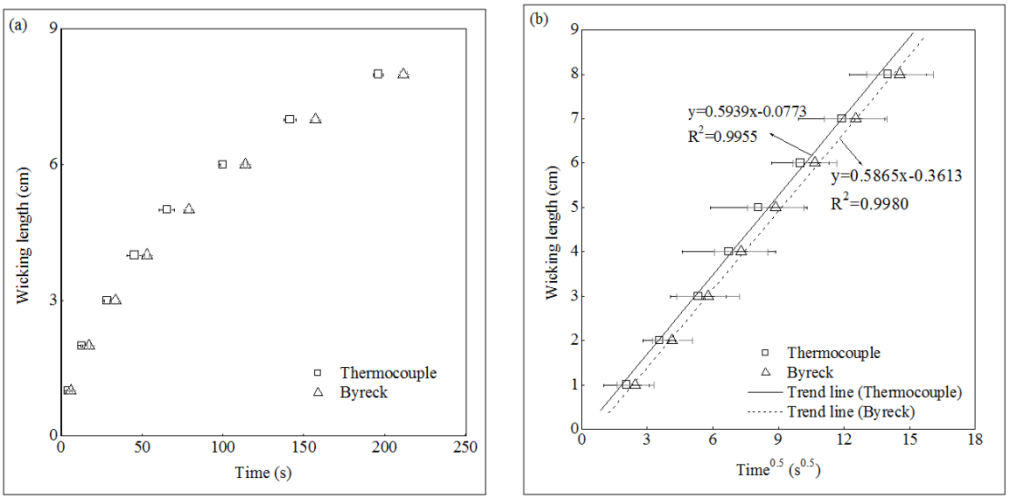

Figure 4.14 Comparison of the results of the two measurements for cotton/polyester fabric (C/P-2) in the bias direction: (a) Relationship between the wicking length and time; (b) Relationship between wicking length and square root of time.

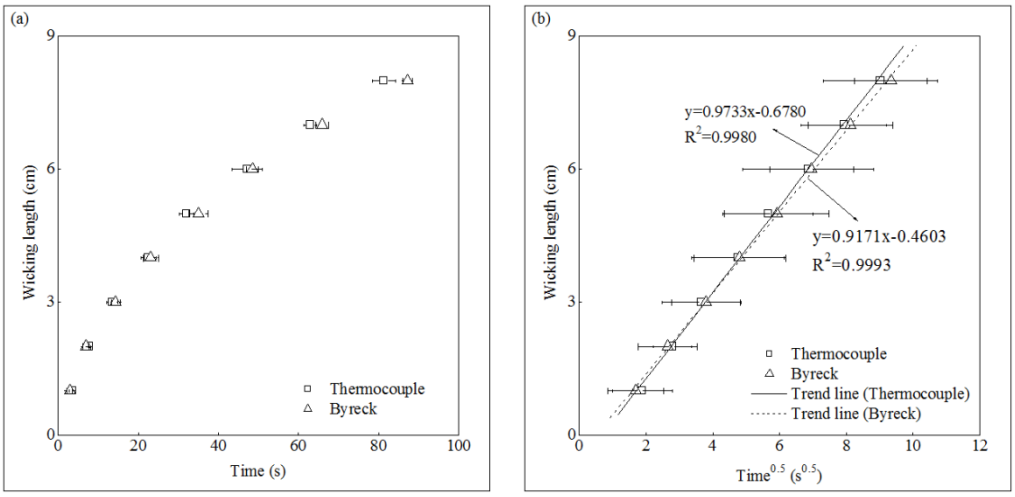

Figure 4.15 Comparison of the results of the two measurements for cotton knit fabric (C-k) in the warp direction: (a) Relationship between the wicking length and time; (b) Relationship between wicking length and square root of time.

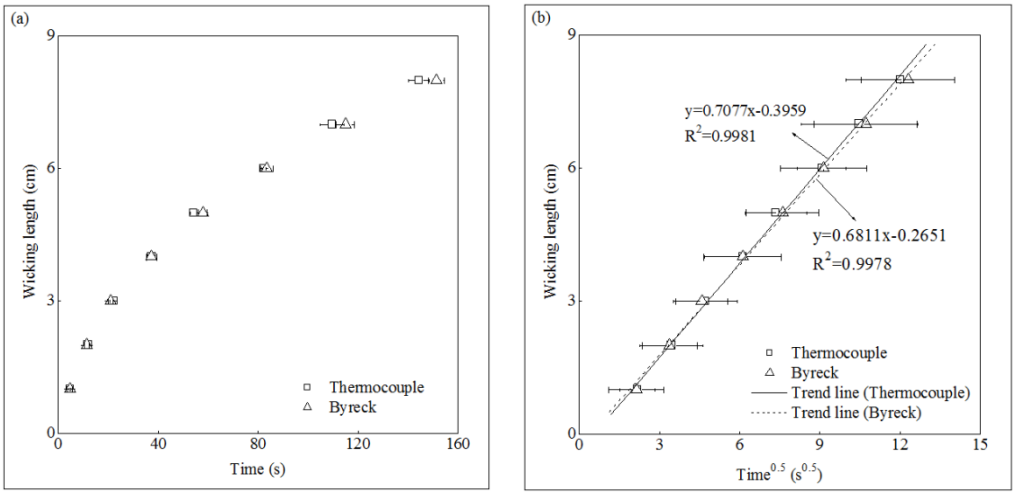

Figure 4.16 Comparison of the results of the two measurements for cotton knit fabric (C-k) in the weft direction: (a) Relationship between the wicking length and time; (b) Relationship between wicking length and square root of time.

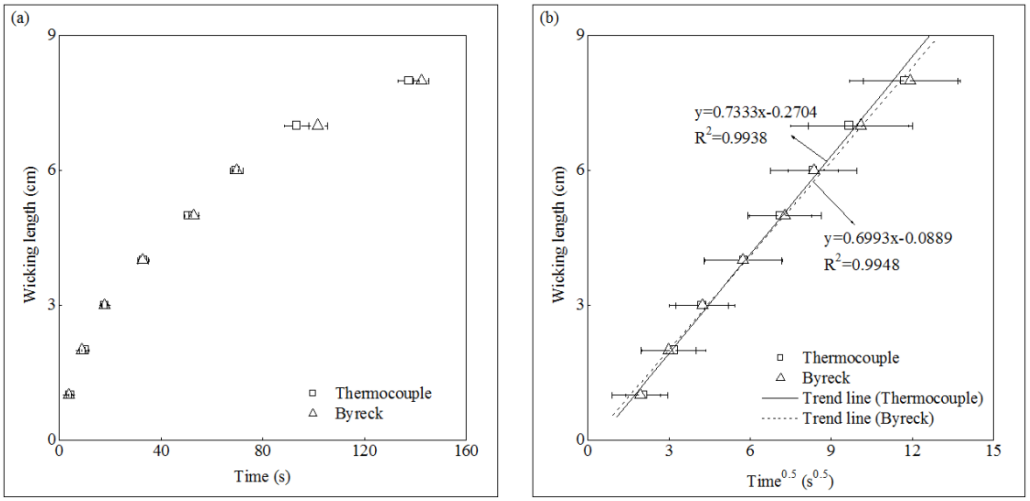

Figure 4.17 Comparison of the results of the two measurements for cotton knit fabric (C-k) in the bias direction: (a) Relationship between the wicking length and time; (b) Relationship between wicking length and square root of time.

The comparison of the wicking coefficient results of all samples by both methods are summarized in Figure 4.18. From this figure, it is evident that the wicking

coefficients determined for each fabric are very consistent between the two measurement methods. It can therefore be concluded that our thermocouple array technique is suitable for tracking liquid movement through fabrics. The data generated by the thermocouples also demonstrate the linear relationship between wicking length and the square root of wetting time predicted by the Washburn equation. Based on these results, we are confident that the thermocouple array technique can be used in place of the Byreck method to follow the flow of water within fabrics.

Table 4.2 Wicking coefficients ($cm/s^{0.5}$) obtained for fabric samples in three directions with two methods.

Fabric	Method	Warp	Weft	45° bias
C	Thermocouple	0.3099	0.2433	0.3259
	Byreck	0.3084	0.2493	0.3243
	ΔW (%)	0.4864	2.4067	0.4934
C/P-1	Thermocouple	0.4618	0.3202	0.4530
	Byreck	0.4660	0.3021	0.4526
	ΔW (%)	0.9013	5.9914	0.0884
C/P-2	Thermocouple	0.5915	0.5618	0.5939
	Byreck	0.5839	0.5391	0.5865
	ΔW (%)	1.3016	4.2107	1.2617
C-k	Thermocouple	0.9733	0.7077	0.7333
	Byreck	0.9171	0.6811	0.6993
	ΔW (%)	6.1280	3.9054	4.8620

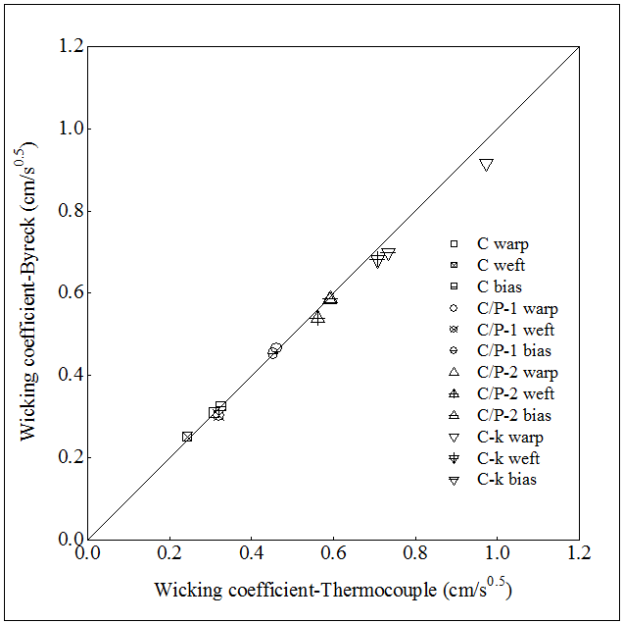

Figure 4.18 Comparison of wicking coefficient results of different fabric samples in three directions from the thermocouple and Byreck method.

4.4.2 Predicting water content from equilibrium temperature of fabric

The relationship between the water content and the temperature of each fabric samples during the drying process is shown in Figure 4.19. For cotton woven fabric (C), the fabric temperature exhibits very little change until the water content approaches approximately 35%, at which point the temperature increases significantly with further decreases in the fabric's water content. These results reflect a typical drying process. In the first period, the free water at fabric surface evaporates. The drying rate is determined by the diffusion of water vapor from the saturated surface of the fabric through a stationary air film into the air stream. This is the constant rate period which it will maintain for a period of time. Eventually the water content of the material drops to a level known as the critical water content, and there is little free water, then water from the inside of the fabric will transport to the surface and evaporate, until the fabric is dry.

This is the falling rate period [25-27]. In this cotton fabric, 35% water content is evidently the critical water content, which refers to the water content of the fabric at the end of the constant period when the falling rate period begins. Above this level, drying occurs in the constant rate period and fabric temperature is approximately constant, whereas below this level, drying enters the falling rate period and the temperature increases greatly with decreasing water content. The critical water content of cotton/polyester fabric (C/P-1, C/P-2) is about 7%, and for the cotton knit fabric, it is about 35%, too. For polyester knit fabric, the critical water content is about 2%. The differences in critical water content are due to the fiber content of fabric. The cotton fabrics (C and C-k) have the highest critical water content, which is caused by more water absorbed by cotton fabric, as well as yarn and fiber. It takes much time for cotton yarn and fiber to release absorbed water and therefore the critical water content is higher than others.

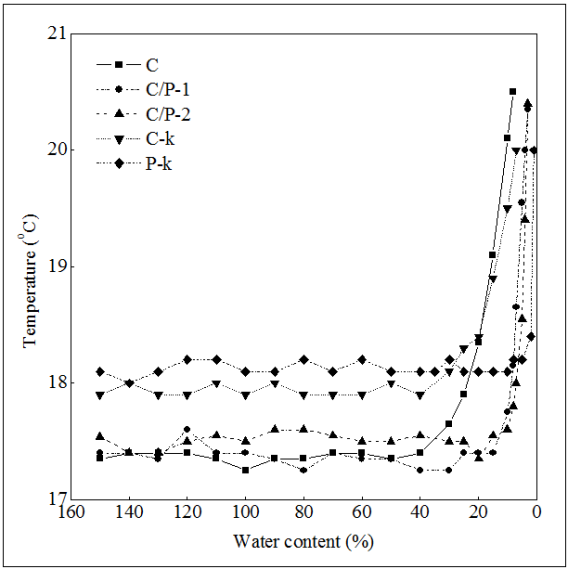

Figure 4.19 Relationship between water content and fabric temperature during the drying process of all fabric samples.

Figure 4.20 presents results concerning the relationship between the temperature difference and the water content of cotton fabric at equilibrium. In this figure, the data points labeled “Weight” represent temperature difference calculated by subtracting fabric temperature shown in Figure 4.19 from room temperature, while the points labeled “C-1” to “C-6” represent the results of thermocouple measurements from six replicate trials. These results demonstrate that the measured temperatures and weights are highly reproducible and that thermocouple results are consist with the weight results. At low values of temperature difference, the slope of the plot between water content and temperature difference is quite small, whereas this slope increases significantly at temperatures above approximately 3℃, corresponding to the water content of about 35%.

Based on the analysis of critical water content, Figure 4.20 can be divided into two parts, as shown by the two regression lines. When temperature difference reaches to 3℃, the water content of fabric varies greatly, and during this process, it is difficult to predict water content only by temperature changes of fabric. However, if temperature difference is below 3℃, the relationship between the water content and temperature difference of each segment is highly in agreement with the regression lines plotted by “Weight” in the experimental trial. The relationship between temperature difference and water content of cotton fabric has been verified. From the temperature difference, the dry and wet conditions of fabric segment can be obtained, and moreover, the water content of fabric segment can be estimated. We therefore conclude that the measured temperature difference between the fabric and ambient can be used to estimate the water content of the fabric, provided the water content of the fabric is below the critical equilibrium water content for the fabric.

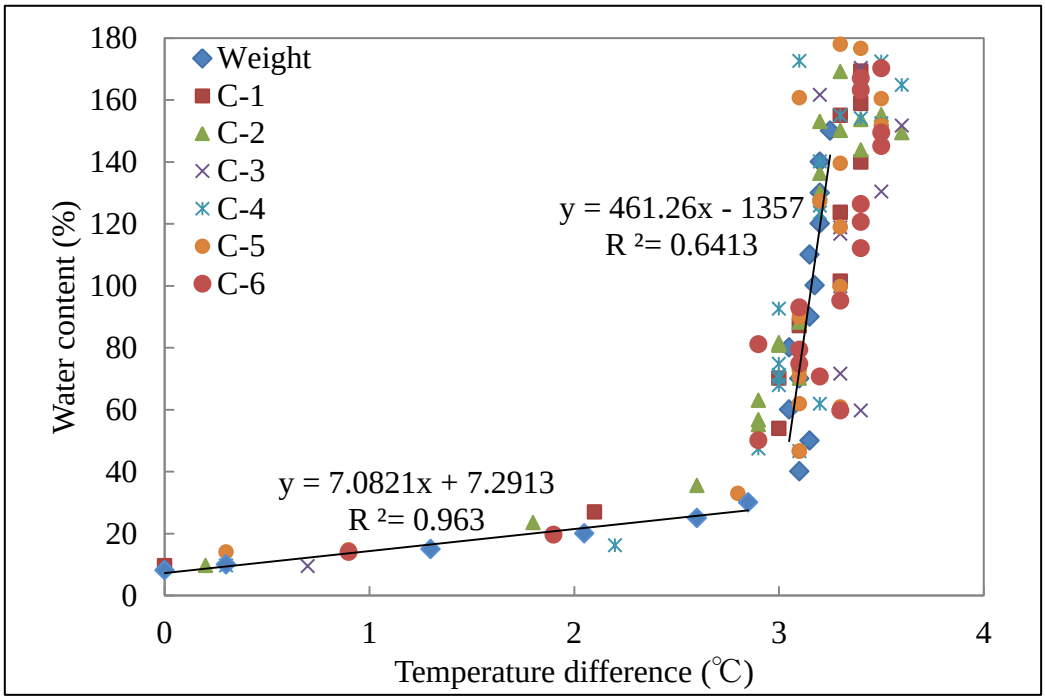

Figure 4.20 Comparison of results obtained by weighing method and thermocouple array method.

4.5 Conclusion

A new method has been proposed for the measurement of in-plane capillary water flow within fabrics. This technique, using data acquired from a series of thermocouples, is capable of automatically tracking the wicking length versus time. The wicking coefficients obtained by this new method were compared with those found using Byreck method, and the accuracy of the thermocouple method was verified. As the measurement thermocouples are physically small, removable and flexible, this method can be applied to many different kinds of textile structures. Moreover, this method can be used to measure the wicking length with respect to time without the addition of dye to the liquid.

In further trials, the relationship between temperature difference and water content was found based on physically weighing fabric specimens and the critical water content was obtained. When the water content of cotton fabric was above the critical water content of about 35%, the temperature difference was essentially constant. However, below this water content, the temperature difference increased rapidly as the water content decreased. Based on these investigations, it appears that it is possible to estimate the water content of fabrics from the thermocouple temperature measurements, so long as the water content of the fabric is lower than the critical value for that material. This method and the associated apparatus are considered to be applicable to many different areas of fabric analysis, including the assessment of wetting in diapers and the dispersion of sweat in sportswear.

References:

1. Erik K. Wetting and wicking. *Text. Res. J.* 1996; 66: 660-668.
2. Hsieh YL. Liquid transport in fabric structures. *Text. Res. J.* 1995; 65: 299-307.
3. Rajagopalan D, Aneja AP and Marchal JM. Modeling capillary flow in complex geometries. *Text. Res. J.* 2001; 71: 813-821.
4. Fangueiro R, Filgueiras A, Soutinho F et al. Wicking behavior and drying capability of functional knitted fabrics. *Text. Res. J.* 2010; 80: 1522-1530.
5. Patnaik A, Rengasamy RS, Kothari VK et al. Wetting and wicking in fibrous materials. *Text. Prog.* 2006; 38: 1-105.
6. Kawase T, Sekoguchi S, Fujii T, et al. Spreading of liquids in textile assemblies: Part I: Capillary spreading of liquids. *Text. Res. J.* 1986; 56: 409-414.
7. Wang N, Zha AX and Wang JX. Study on the wicking property of polyester filament yarns. *Fibers Polym* 2008; 9: 97-100.
8. Jiang XY, Zhou XH, Weng M, et al. Image processing techniques and its application in water transport through fabrics. *J Fiber Bioeng Inform* 2010; 3: 88-93.
9. Perwuelz A, Mondon P and Caze C. Experimental study of capillary flow in yarns. *Text. Res. J.* 2000; 70: 333-339.
10. Lord PR. A comparison of the performance of open-end and ring spun yarns in terry toweling. *Text. Res. J.* 1974; 44: 516-522.
11. Merve KO, Banu N and Cevza C. A study of wicking properties of cotton-arcylic yarns and knitted fabrics. *Text. Res. J.* 2011; 81: 324-328.
12. Esra C, Alex JF and Steven BW. Fibrous structures with designed wicking properties. *Text. Res. J.* 2007; 77: 256-264.
13. Rossi RM, Stampfli R, Psikuta A, et al. Transplanar and in-plane wicking effects in

sock materials under pressure. *Text. Res. J.* 2011; 81: 1549-1558.

14. Su CI, Fang JX, Chen XH, et al. Moisture absorption and release of profiled polyester and cotton composite knitted fabrics. *Text. Res. J.* 2007; 77: 764-769.
15. Japanese Industrial Standard L 1907: 1994. Test method of water absorbency of textiles-5.1.2, Byreck method.
16. Din 53924. *Velocity of suction of textile fabrics in respect of water- method determining the rising height*. Berlin: Deutsches Institut fur Normung, 1997.
17. Yoneda M and Niwa M, Measurement of in-plane capillary water flow of fabrics. *Sen'i Gakkaishi* 1992; 48: 288-298.
18. Hsieh YL and Yu B. Liquid wetting, transport, and retention properties of fibrous assemblies. Part I: water wetting properties of woven fabrics and their constituent single fibers. *Text. Res. J.* 1992; 62: 677-685.
19. Bayramli E and Powell RL. Experimental investigation of the axial impregnation of oriented fiber bundles by capillary forces. *Colloids Surf* 1991; 56: 83-100.
20. Ito H and Muraoka Y. Water transport along textile fibers as measured by an electrical capacitance technique. *Text. Res. J.* 1993; 63: 414-420.
21. Babu VR and Koushik CV. Capillary rise in woven fabrics by electrical principle, *Indian J Fibre Text Res*; 2011; 36: 99-102.
22. Zhu CH and Takatera M. Change of temperature of cotton and polyester fabrics in wetting and drying process, *J Fiber Bioeng Inform* 2012; 5:433-446.
23. Mhetre S and Parachuru R. The effect of fabric structure and yarn-to-yarn liquid migration on liquid transport in fabrics. *J Text Inst* 2010; 101: 621-626.
24. Nyoni AB. Liquid transport in Nylon 6.6 woven fabrics used for outdoor performance clothing. In: Vassiliadis S (eds) *Advances in modern woven fabrics*

technology. Rijeka: InTech, 2011, pp.211-240.

25. Haghi AK. Thermal analysis of drying process: A theoretical approach. *J Therm Anal Calorim* 2003; 74: 827-842.
26. Richard S. Factors affecting the drying of apparel fabrics. Part I: Drying behavior. *Text. Res. J.* 1958; 28: 136-144.
27. Sasaki S, Kubo J. Drying performance of cloths hung in a thermostatic oven (Part 2) The relationship between the drying rate and the surface temperature of wet cloths. *Nakumura Gakuen Univ* 1980; 13: 129-133.

Chapter 5

Effect of fabric structure and yarn on capillary liquid flow within fabrics

Chapter 5 Effect of fabric structure and yarn on capillary liquid flow within fabrics

5.1 Introduction

Capillary rise in fibrous structures is frequently observed in many fields, such as wetting and wicking in textiles, paper and porous media [1-5]. Wetting is the displacement of a solid-air interface with a solid-liquid interface. In a broader sense, the term “wetting” is used to describe the replacement of a solid-liquid or liquid-air interface with a liquid-liquid interface, and a solid-air interface with a solid-solid interface. The transport of a liquid into a fibrous assembly, such as yarn or fabric, may be caused by external forces or by capillary forces only. Spontaneous transport of liquid driven into a porous system by capillary forces is termed “wicking”. Because capillary forces are caused by wetting, wicking is a result of spontaneous wetting in a capillary system [6].

There are many researches on the wetting and wicking on fabrics. Three major techniques have been used to analyze liquid flow through yarns and fabrics quantitatively. The first is measuring the capillary flow of a colored liquid and recording its height versus time [7-13]. The conventional Byreck method is based on this technique. The CCD camera and image analysis techniques are also used to record the height with respect to time. The second technology consists of measuring weight variation with a balance during capillary wicking [14-15]. The last is to set liquid-sensitive sensors regularly along the fabrics or yarns [16-20]. The liquid-sensitive sensors are usually for measuring humidity, electrical capacitance, temperature and so

on. In essence, liquid flow within textile structures is typically studied in one of the two ways, either by measuring the liquid front height or by measuring the weight of liquid absorbed as a function of time.

Wicking plays an important role in textile applications, especially in the design and use of sports wears and industrial uniforms, as well as in various processes such as dyeing, finishing and filtration. Many researches of wicking phenomenon have been investigated on the use of these techniques. Russell et al [21] investigated in-plane anisotropic liquid absorption in nonwoven fabrics, using variations in electrical capacitance to monitor changes in the liquid absorbed by a fabric as a function of time. Benltoufa et al [22] studied the capillary rise in macro and micro pores of a jersey knitting structure. Merve et al [23] studied the wicking properties of cotton-acrylic yarns and knitted fabrics, and found that the wicking abilities of yarns and fabrics increased with the increase in their acrylic content and with the use of coarse yarns. Perwuelz et al [12] studied the capillary flow in polyester and polyamide yarns and glass fibers using a technique based on analyzing CCD images taken during the capillary rise of colored liquid in yarns. They found that the kinetics of capillary rise always follow the Washburn equation, but attribute the great dispersion of the experimental results along the yarns to the yarn heterogeneity of the inter-filament space. Yanilmaz et al investigated the relationship between different knitted structures and some thermophysiological comfort parameters by measuring the wicking height, wicking weight, and transfer wicking ratio [24]. Hsieh [7] discussed wetting and capillary theories and applications of pore structures to the analysis of liquid wetting and transport in capillaries and fibrous materials. He found that for a fibrous material to effectively transport a liquid, the fibers must be easily and thoroughly wetted by the

liquid. Moreover, the significance of fiber properties had been demonstrated. Mhetre et al [25] carried out wicking experiments on a range of cotton and polyester fabrics, which had different yarn sizes, thread spacing, and yarn types. The results showed that the wicking in fabrics was determined by the wicking behavior of the yarn, the thread spacing and the yarn migration rate, which was the ability of liquid to migrate from longitudinal to transverse threads and from transverse back to longitudinal threads.

However, there is little research on predicting the liquid transport property of a fabric from the specifications of the fabric. In this paper, we studied wicking length versus time of different woven fabrics using the thermocouple array technology [19]. We also investigated the influence of fabric structural parameters on wicking behavior, including fiber content, yarn count and weave density.

5.2 Basic theory

The theory of wicking was introduced in Chapter 2.

When fabric is immersed in a liquid, the liquid first starts to move along longitudinal yarns. When the flow front encounters transverse yarns, some of the liquid in the longitudinal yarns will move into the transverse yarns. The transferred liquid remains in the segments of transverse threads, and it may act as a new reservoir for the wicking process in longitudinal yarns. Because of these additional reservoirs, the rate of liquid wicking in longitudinal yarns can go up. Liquid can also get stored in the inter-yarn spaces, which can also act as additional reservoirs [25, 26].

5.3 Experimental

5.3.1 Test apparatus

The wicking experiments were conducted on the thermocouple array technology [19, 27]. Figure 5.1 shows diagrams of the test apparatus. The apparatus consisted of 12 thermocouple measurement points set 5 mm apart and sitting on foam polystyrene for heat insulation. The thermocouples were made from copper and constantan element wires with the diameter of 0.1mm. The wetted end of the fabric strip or yarn was clipped to a weight. As the fabric or yarn absorbed water, changes in temperature were measured by the thermocouple array.

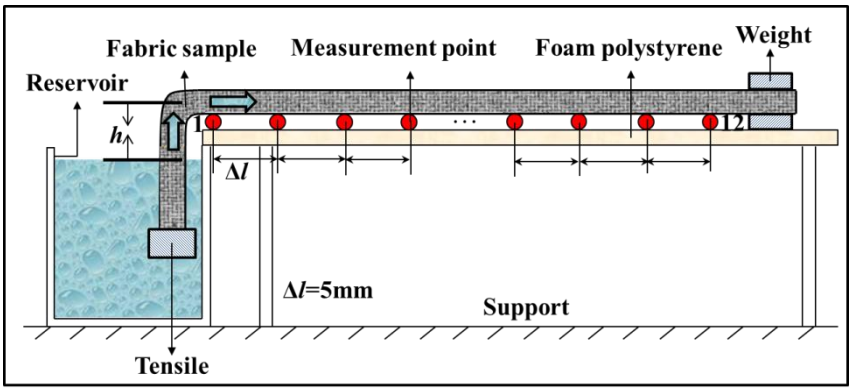

Figure 5.1 Schematic of modified thermocouple method.

5.3.2 Test samples

The fabric samples used in this experiment were woven by a sample rapier loom. We used 100% cotton yarn as the warp yarn, and a range of plain fabrics were woven by changing fabric structural parameters, such as the kinds of weft yarn, the weave density and the weft yarn count. Tables 5.1 and 5.2 give the weaving parameters and physical properties of each sample.

Table 5.1 Weaving parameters of fabric samples.

Fabric sample	Warp yarn	Weft yarn	Warp weave density ($inch^{-1}$)	Weft weave density ($inch^{-1}$)
C-1	100% cotton, 13tex ($2/80^S$), 280 t/m	100% cotton, 13tex ($2/80^S$), 280t/m	120	10
C-2				20
C-3				30
C-4				40
C-5				60
C-6				80
C-7				90
C/P-1		C:P =50:50, 19tex, 862 t/m		60
C/P-2		C:P =50:50, 29.5tex, 692 t/m		60
P		100% polyester, 29.5tex ($2/40^S$), 362 t/m		60

C: P in Table 5.1 refers to “cotton: polyester”.

t/m: Unit of yarn twist, means “twists of yarn per meter”.

These fabrics were first pretreated to remove adhesives and impurities on the fabrics or yarns that were used in the manufacturing process. We did pretreatment as follows: 1) boiling twice in the water bath with a water temperature of 80 ± 2 ℃; 2) boiling once with a detergent, with the dispersion of a detergent (Polyoxyethylene lauryl ether, Kao Corporation EMULGEN 108) over water of 1g/10L, in a water bath of 80 ± 2 ℃. After each boiling, the fabric samples were washed carefully with water. Then we dried these samples under standard conditions for 24 hours.

Table 5.2 Physical properties of fabric samples.

Fabric sample	Thickness (mm)	Area density (g/m^2)	Porosity (%)
C-1	0.916	81.22	94.24
C-2	0.749	86.79	92.47
C-3	0.701	93.85	91.31
C-4	0.695	104.23	90.26
C-5	0.660	123.43	87.86
C-6	0.628	135.01	86.04
C-7	0.618	139.24	85.37
C/P-1	0.774	115.21	89.80
C/P-2	0.850	158.66	87.21
P	0.830	186.54	83.72

Test fabric specimens (20 by 3 cm) were carefully cut from each fabric at varying locations along the warp and weft directions. These fabric specimens were used for measuring wicking length with respect to time. We tested eight samples for each direction of each fabric and determined the average and standard deviations.

Yarn specimens were prepared from the corresponding fabric. The weft sample was prepared as follows. First we cut a fabric strip of length 20 cm in the weft direction and width 1 cm in the warp direction. Then we took out the warp yarns from the strip, but left the two ends consisting of the fabric structure. We left 0.5 cm of fabric on one end to use for clipping the weight, and left 5 cm on the other end to be fixed to keep the yarn taut during the experimental trial. We pulled out some weft yarns from both sides and made the yarn sample 0.5cm wide eventually. The prepared yarn specimen is shown in

Figure 5.2. We tested eight yarn samples for weft direction of all the fabrics and determined the average and standard deviations. For the warp direction, similar methods were used to prepare the specimens. As we used the same warp yarn with the same weave density, we just made eight samples of C-1 fabric, and calculated the average and standard deviation.

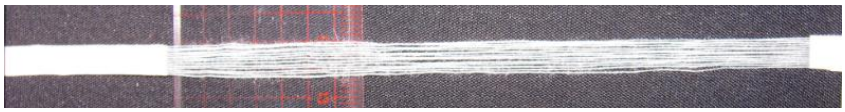

Figure 5.2 A yarn specimen for experimental trial.

Experiments were performed at a constant temperature and relative humidity of 20 ± 1 ℃ and 65 ± 2% RH. The wicking coefficients were determined for all the fabrics and yarns by fitting the length-time data to the Washburn equation.

5.4 Results and discussion

5.4.1 Effect of weave density on the wicking coefficient of fabric

Figure 5.3 shows the average wicking coefficients of the cotton fabric in warp and weft directions for a range of weft weave densities. For the same fabric, the wicking coefficients are different along the warp and weft directions. This is the anisotropy of the fabric. The wicking coefficient went down with increasing weft weave density both in the warp and the weft directions. This can be explained by the relationship between weave density and the effective capillary radius *R*. Because these fabrics were woven with the same yarn, the percentage of fibers per unit width increased as the weft density increased, which would lower the average effective capillary radius. According to the Washburn equation, the wicking coefficient decreased. However, in the weft direction, the wicking coefficient will not rise limitlessly with decreasing weft weave density. As shown in this figure, when weft weave density reduced to 10 per inch, the wicking coefficient in the weft direction decreased.

The gain in wicking coefficient [25], ΔW, was determined using

$$\Delta W = \frac{W_F - W_Y}{W_Y} \times 100, \tag{5.1}$$

where W_F is the wicking coefficient of the fabric, and W_Y is the wicking coefficient of the yarn.

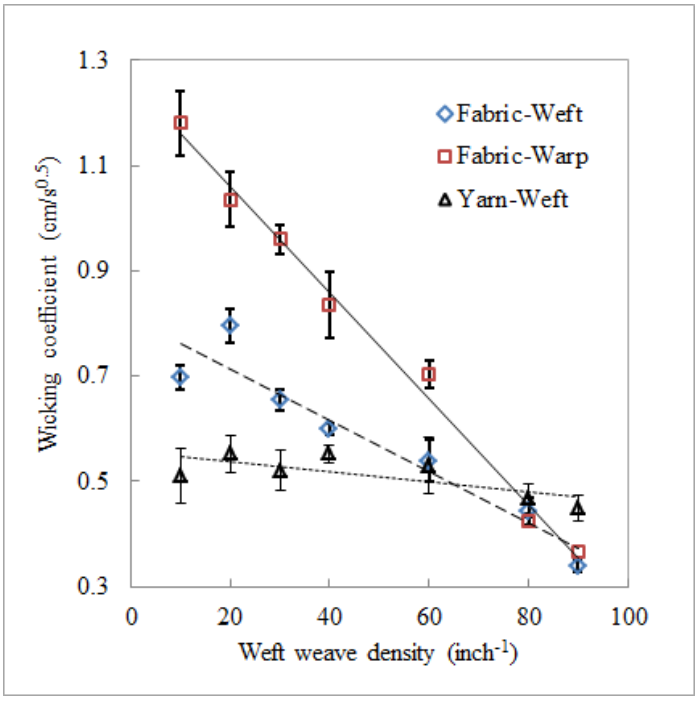

Figure 5.3. Wicking coefficient against weft weave density for cotton fabric.

Table 5.3 shows the gain in wicking coefficient of fabrics in the warp and weft directions. The highest gain was observed in the weft direction of the C-2 fabric, followed by the weft direction of the C/P-2 fabric and the C-1 fabric. The gain in wicking coefficient is influenced by the weave density, which shows the same result as Figure 5.3 analyzed above. Instead of studying two different weave densities as Mhetre [25] did, we examined the effect of the wicking coefficient for fabrics with a range of weave densities, and found the wicking coefficient decreased with increasing weave density. This means that the liquid stored in the inter-yarn plays an important role, as noted by Mhetre [25]. Moreover, it was found that the weft yarn had a positive effect on the wicking coefficient of fabric when the weave density was low (less than 40 per inch). This may be the reason for the effective capillary radius mentioned above. The effect of wicking performance for yarn can be used to predict the capillary property of fabrics.

Table 5.3 Gain in wicking coefficients of fabrics for warp and weft yarns and fabrics.

Fabric sample	Gain in wicking coefficient (%)	
	Warp	Weft
C-1	36.41	36.45
C-2	19.67	44.28
C-3	10.92	25.68
C-4	–3.40	8.39
C-5	–18.64	1.51
C-6	–51.01	–5.42
C-7	–57.84	–24.32
C/P-1	–37.88	0.54
C/P-2	–43.30	40.32
P	–37.79	25.77

Figure 5.3 also presents the wicking coefficients of yarns for different densities. The coefficients have almost the same value until a density of 60 per inch. This is mainly because for lower weave density, the capillary water flow between yarns can be neglected; the capillary phenomenon is driven only because of the yarn. The same cotton yarn shows the same wicking rate, as it should. However, when the density is high, reaching 80 per inch, the wicking coefficient tends to decrease. To explain this, the yarn crimp *c* for these fabrics was calculated using Equation (5.2) [28],

$$c(\%) = \frac{l_Y - l_F}{l_F} \times 100, \tag{5.2}$$

where l_F is the distance between two points on a yarn as it lies in the fabric, and l_Y is the straightened distance of the yarn.

The relationship between crimp and wicking coefficient of weft yarn is shown in Figure 5.4. With the increase of yarn crimp, the wicking coefficient shows decreasing. The yarn crimps for weft weave density of 80 and 90 per inch are 3.86% and 3.97% respectively, larger than that for lower weave density. The larger crimps caused the longer wicking path, and therefore the wicking coefficients decreased at both 80 and 90 per inch. As the same warp yarn and warp weave density are used for the sample fabrics, the wicking coefficient of warp yarn is the same, 0.865 cm/s$^{0.5}$. Moreover, as shown in Figure 5.3, the wicking coefficients are higher than those of their constituent yarns with low weft densities.

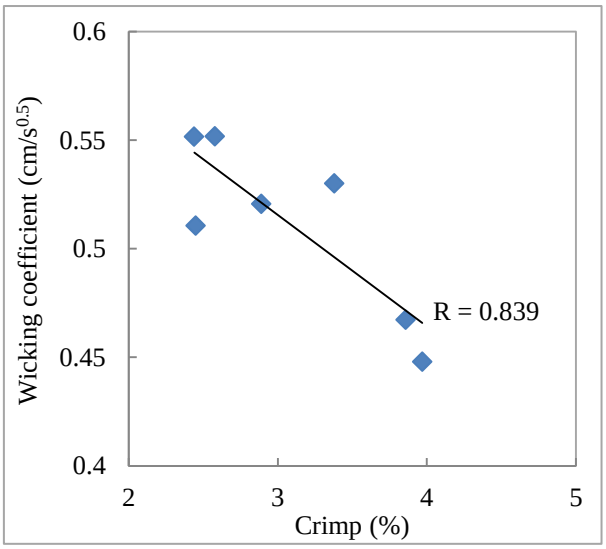

Figure 5.4 The relationship between crimp and wicking coefficient of weft yarn.

To investigate the effect of inter-fiber distance, the porosity (ϕ) [7] of a range of cotton fabrics was calculated using

$$\phi = 1 - \frac{\text{bulk volume}}{\text{medium volume}} = 1 - \frac{\rho_b}{\rho_s}. \tag{5.3}$$

Here ρ_b and ρ_s are the bulk and medium densities, respectively. In the case of

fabrics, ρ_b is the fabric density and ρ_s is the fiber density. Fabric density can be calculated with

$$\rho_b = \frac{\text{fabric weight (g/cm}^2)}{\text{thickness (cm)}}. \tag{5.4}$$

The calculated porosity is shown in Table 5.2. Figure 5.5 shows the relationship between porosity and wicking coefficient of cotton fabrics. As the porosity of fabric increases, the wicking coefficient increase. This is probably because the fiber space increases with rising porosity, providing the effect channel for water transport; this can enhance the wicking coefficient.

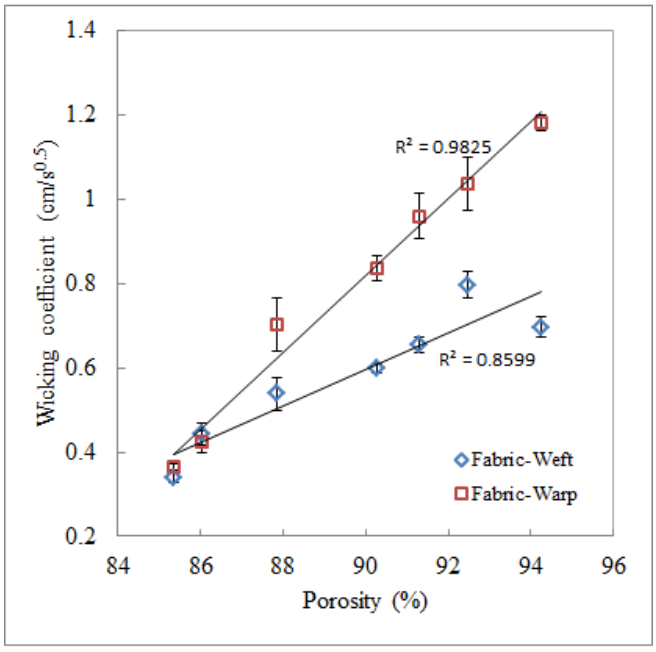

Figure 5.5 Relationship between porosity and wicking coefficient for a range of cotton fabrics.

5.4.2 Effect of weft yarn on the wicking coefficient of fabric

Figure 5.6 shows the relationship between wicking coefficients of fabrics and different yarns used in the weft direction (C-5, C/P-1, C/P-2, P in Table 5.1). Four kinds of weft yarns were used, with the same weft weave density of 60 per inch. The correlation coefficients of weft yarn and fabric on the warp and weft directions are 0.814 and 0.686 respectively. However, they do not have any significant difference for level of significance of less than 0.05. The wicking coefficient of cotton yarn (C-5) is larger than others, and the fabrics show the same trends with yarns.

For different yarn counts (C/P-1 and C/P-2), from the scanning electron microscope (SEM) images of the cross sections and longitudinal sections of the yarns in Figure 5.7 and 5.8, the fiber for the weft yarn of C/P-1 fabric is thicker than that of C/P-2 weft yarn, which causes the inter-fiber space bigger than the other one, and results in a higher wicking coefficient.

Figure 5.6 shows that although the wicking rate of cotton-polyester blended (C/P-1) weft yarn is higher than that of polyester (P) weft yarn, the wicking coefficients of the fabrics are almost the same. This indicates that the wicking in fabric may be determined not only by the coefficient of the yarns but also the effect of yarn on the whole fabric. As shown in Table 5.3, the gain in the wicking coefficient of cotton-polyester blended fabric (C/P-1) in the weft direction is smaller than that of polyester fabric (P). The polyester yarn plays a positive role in the capillary properties of fabric in the weft direction.

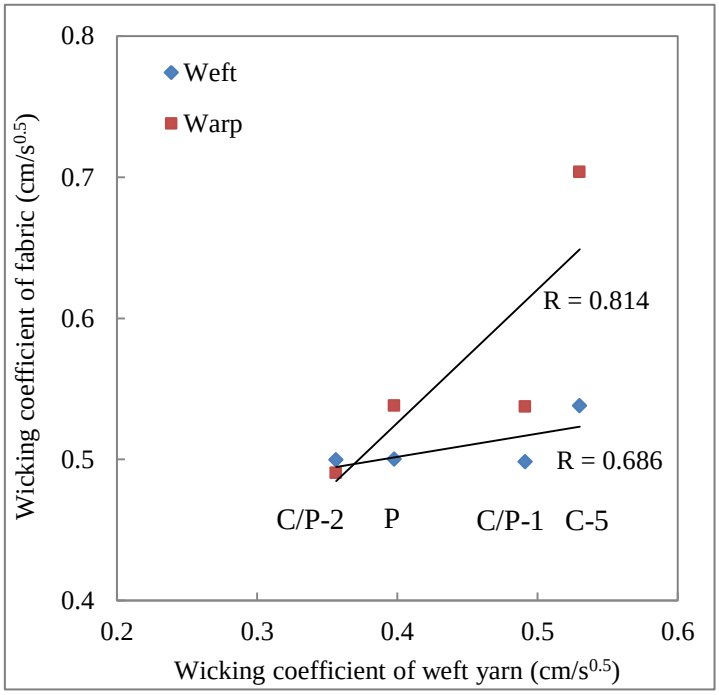

Figure 5.6 Wicking coefficients of different fabrics versus wicking coefficients of weft yarns.

Figure 5.7 shows the SEM images of the cross sections of the four yarns, and Figure 5.8 shows the SEM images of their longitudinal sections. Compared with the circular cross section of the polyester fiber, the cross section of the cotton fiber is irregular with more inter-fiber space, and the water diffusion is higher than in other fibers. The inter-fibers in the cotton-polyester blended yarn are close to each other, which reduced the effective capillary radius; therefore, the wicking coefficient of cotton polyester blended yarn is smaller than that of cotton yarn. Moreover, from the longitudinal pictures in Figure 5.8, both cotton and polyester yarns are ply yarns with low twist levels, and the cotton-polyester blended yarns are spun yarns with higher twist levels. Both cotton and polyester yarns have less twist, which keeps the yarns more open, and hence effective capillary radius is larger for open yarn. Therefore, the wicking

coefficient of cotton yarn is the highest.

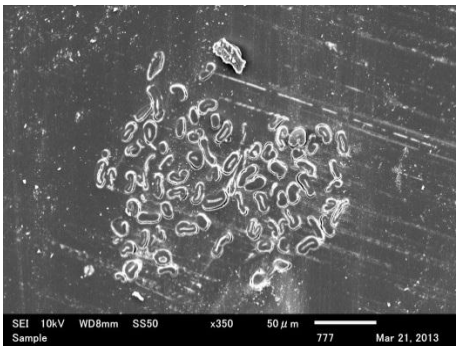

(a)

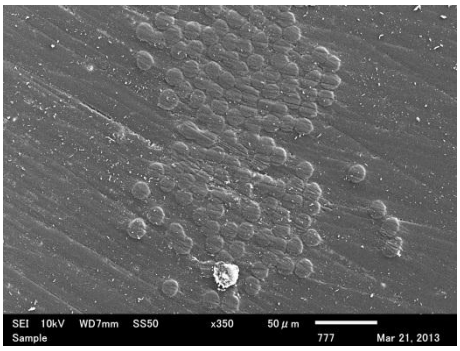

(b)

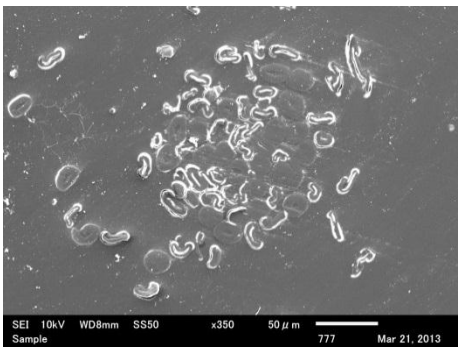

(c)

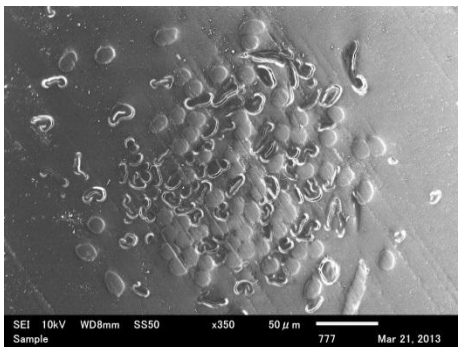

(d)

Figure 5.7 SEM images of cross sections for four yarns: (a) cotton yarn; (b) polyester yarn; (c) weft yarn for C/P-1 fabric; (d) weft yarn for C/P-2 fabric.

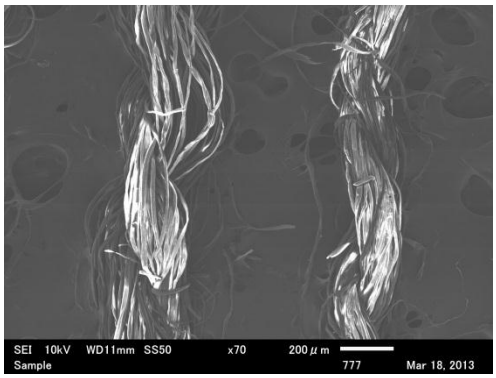

(a)

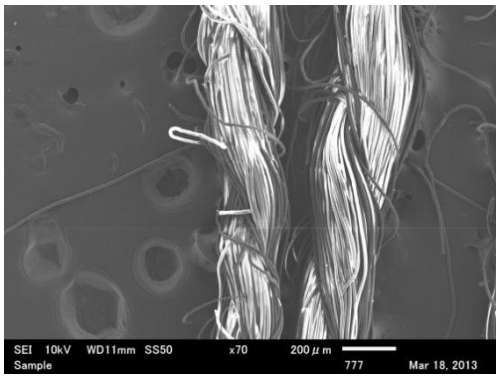

(b)

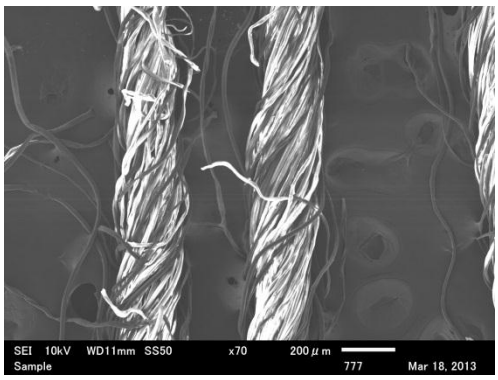

(c)

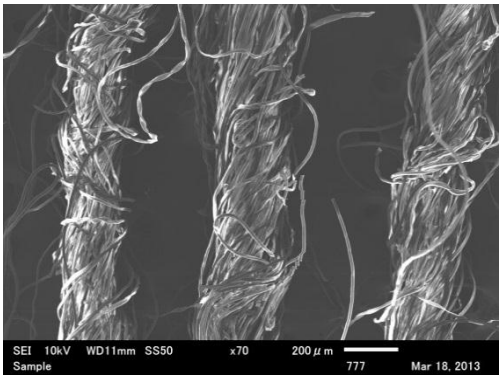

(d)

Figure 5.8 SEM images of longitudinal sections for four yarns: (a) cotton yarn; (b) polyester yarn; (c) weft yarn for C/P-1 fabric; (d) weft yarn for C/P-2 fabric.

5.5 Conclusion

We studied the relationship between the wicking coefficients of fabrics and yarns. A range of plain fabrics were woven, using the same warp yarn but changing the fiber content, yarn count and weave density of weft yarn.

A thermocouple array technology was used to determine the wicking coefficients of these fabrics and yarns. The wicking coefficients were determined by fitting the wicking length and time to the Washburn equation. The results for different weave densities of cotton fabrics showed that the wicking coefficient decreased with increasing weave density both in the warp and weft directions. The fabric with largest weave density showed the lowest wicking coefficient because it had the smallest effective capillary radius. The relationship between porosity and wicking coefficient showed the same trend for different weave densities: as the porosity of fabric increased, so did the wicking coefficient. The gain in wicking coefficient showed that weft yarn had a positive effect on the fabrics at lower weft density. The wicking coefficients of cotton yarns with different weave densities showed the same value before 60 per inch. However, if the weft density was high, reaching 80 or 90 per inch, the wicking coefficients decreased because of the yarn crimps.

Four kinds of yarns were used in this experiment to study the effect of fiber content on the capillary property, and the 100% cotton yarn and the corresponding fabric showed the highest wicking coefficient. For different yarn counts, the larger inter-fiber space had a positive effect on the capillary property of the yarn, which was confirmed from the SEM images of the cross sections and longitudinal sections of the yarns. The SEM pictures also showed the role of twist in the wicking influence factor as it relates

to fibers. We found that the wicking rate was higher for larger inter-fiber space and fewer twist yarns.

References:

[1] Bayramli E, Powell RL. Experimental investigation of the axial impregnation of oriented fibre bundles by capillary forces. *Colloids Surf.* 1991; 56: 83-100.

[2] Danino D, Marmur A. Radial capillary penetration into paper: limited and unlimited liquid reservoirs. *J. Colloid Interface Sci.* 1994; 166: 245-250.

[3] Hodgson KT, Berg JC. The effect of surfactants on wicking flow in fiber networks. *J. Colloid Interface Sci.* 1988; 121: 22-31.

[4] Kamath YK, Hornby SB, Weigmann HD, Wilde MF. Wicking of spin finishes and related liquids into continuous filament yarns. *Text. Res. J.* 1994; 64: 33-40.

[5] Liu T, Choi KF. Capillary rise between cylinders. *Surf. Interface Anal.* 2008; 40: 368-370.

[6] Kissa E. Wetting and wicking. *Text. Res. J.* 1996; 66: 660-668.

[7] Hsieh YL. Liquid transport in fabric structures. *Text. Res. J.* 1995; 66: 299-307.

[8] Rajagopalan D, Aneja AP., Marchal JM. Modeling capillary flow in complex geometries. *Text. Res. J.* 2001; 71: 813-821.

[9] Kawase T, Sekoguchi S, Fujii T and Minagawa M. Spreading of liquids in textile assemblies. *Text. Res. J.* 1986; 56: 409-414.

[10] Wang N, Zha AX, Wang JX. Study on the Wicking property of polyester filament yarns. *Fibers Polym.* 2008; 9: 97-100.

[11] Jiang XY, Zhou XH, Weng M, Zheng JJ, Jiang YX. Image processing techniques and its application in water transport through fabrics. *J Fiber Bioeng Inform.* 2010; 3: 88-93.

[12] Perwuelz A, Mondon P, Caze C. Experimental study of capillary flow in yarns. *Text. Res. J.* 2000; 70: 333-339.

[13] Japanese Industrial Standard L 1907: 1994. Test method of water absorbency of textiles-5.1.2, Byreck method.

[14] Hsieh YL, Yu B. Liquid wetting, transport, and retention properties of fibrous assemblies. Part I: water wetting properties of woven fabrics and their constituent single fibers. *Text. Res. J.* 1992; 62: 677-685.

[15] Bayramli E, Powell RL. Experimental investigation of the axial impregnation of oriented fiber bundles by capillary forces. *Colloids Surf.* 1991; 56: 83-100.

[16] Ito H, Muraoka Y. Water transport along textile fibers as measured by an electrical capacitance technique. *Text. Res. J.* 1993; 63: 414-420.

[17] Babu VR, Koushik CV. Capillary rise in woven fabrics by electrical principle, *Indian J. Fibre Text. Res.* 2011; 36: 99-102.

[18] Yoneda M, Niwa M. Measurement of in-plane capillary water flow of fabrics. *Sen-I Gakkaishi* 1992; 48: 288-298.

[19] Zhu CH, Takatera M. Measurement of in-plane capillary water flow of fabrics by thermocouples. 10th WSEAS International Conference on Fluid Mechanics, Italy, 2013.

[20] Zhu CH, Takatera M. Change of temperature of cotton and polyester fabrics in wetting and drying process. *J Fiber Bioeng Inform.* 2012; 5: 433-446.

[21] Russell SJ, Mao N. Apparatus and method for the assessment of in-plane anisotropic liquid absorption in nonwoven fabric. *Autex Res. J.* 2000; 1: 47-53.

[22] Benltoufa S, Fayala F, Nasrallah SB. Capillary rise in macro and micro pores of jersey knitting structure. *J. Eng. Fibers Fabr.* 2008; 3: 47-54.

[23] Merve KO, Banu N, Cevza C. A study of wicking properties of cotton-acrylic yarns and knitted fabrics. *Text. Res. J.* 2011; 81: 324-328.

[24] Yanilmaz M, Kalaoglu F. Investigation of wicking, wetting and drying properties of acrylic knitted fabrics. *Text. Res. J.* 2012; 82: 820-831.

[25] Mhetre S, Parachuru R. The effect of fabric structure and yarn-to-yarn liquid migration on liquid transport in fabrics. *J. Text. Inst.* 2010; 101: 621-626.

[26] Hollies NRS, Kaessinger MM, Watson BS, Bogaty H. Water transport mechanisms in textile materials: Part II: Capillary-type penetration in yarns and fabrics. *Text. Res. J.* 1957; 27: 8-13.

[27] Zhu CH, Takatera M. A new thermocouple technique for the precise measurement of in-plane capillary water flow with fabrics. *Text. Res. J.* Accepted, 2013.

[28] Kang TJ, Choi SH, Kim SM, Oh KW. Automatic structure analysis and objective evaluation of woven fabric using image analysis. *Text. Res. J.* 2001; 71: 261-270.

Chapter 6

Conclusion

Chapter 6 Conclusion

Liquid transport plays an important effect on the comfort of clothing, as liquid transport in fabrics is always accompanied with temperature and humidity changes. In this study, new measurement methods for water transport in fabrics were developed. The new methods were based on the temperature changes in the wetting and drying process, measured by thermocouples.

A multipoint thermocouple-equipped fabric was developed to investigate in detail the conditions that occurred when a droplet of liquid came into contact with fabrics. T-type thermocouples were inserted into cotton and polyester fabrics, with the measurement points located along the warp yarns to form a pattern consisting of two concentric circles with radii of 3 and 6 cm. The results provided useful information regarding temperature changes associated with the wetting and drying process. The temperature on dropped points and circumference points are different from each other for cotton and polyester fabrics, which showed the properties of these fabrics. The method showed possibility for the prediction of wearer discomfort levels resulting from the temperature decline associated with wetted fabrics. Moreover, the woven method for a two-layer thermocouple-equipped fabric was give, and the fabric can be used as garments for temperature measurement and liquid detection in the future.

An automatic measurement method was proposed for in-plane capillary water flow within fabrics. Based on the Lucas-Washburn equation, the new method was used for investigating the relationship between wicking length and wicking time. The measurement device contained an array of nine thermocouple measurement points set 10mm apart and sitting on foam polystyrene for heat insulation. The theory of this

measurement was the fabric temperature at the flow front changed during the process of water absorption because of heat transference associated with both wetting and evaporation. As the fabric initially absorbed water, wetting heat is generated and the local temperature temporarily increased, after which it began to fall down. These temperature changes are used for calculating the wicking time to obtain the wicking coefficient. Compared the wicking coefficients with the results acquired by the horizontal Byreck method, the thermocouple technique was found to be suitable for the precise and automatic measurement of in-plane capillary water flow through fabrics. Moreover, in order to predict water content of fabric for specified points, the relationship between temperature and water content was investigated by rearranging measurement points to the corresponding locations. The results showed that for cotton fabric, below the critical water content (about 35%), fabric temperature changes were relatively large when the water content fell down. It can be used to estimate water content of fabric from temperature changes. This method and the associated apparatus can be applicable to many different areas of fabric analysis, including the assessment of wetting in diapers and the dispersion of sweat in sportswear.

Based on the thermocouple array measurement, the relationship between wicking coefficients of fabrics and yarns were investigated. The results showed that the wicking coefficient went down with increasing weft weave density both in the warp and the weft directions. The results for four kinds of yarns showed that the 100% cotton yarn and cotton fabric had the highest wicking coefficient. Based on scanning electron microscope observation of cross section and longitudinal section of yarns, we discussed the effects of inter-fiber space and yarn twist on the wicking influence factor and found that the wicking rate is higher for larger inter-fiber space and yarns with fewer twists.

These methods, using thermocouples, also showed the possibility for future uses, such as smart clothes for temperature measurement and water content estimation, diaper for urine detection and so on.

Published papers

The dissertation based on following published papers:

1. Chunhong Zhu, Masayuki Takatera, Change of Temperature of Cotton and Polyester Fabrics in Wetting and Drying Process, *Journal of Fiber Bioengineering and Informatics*, 5 (4), pp. 433-446, 2012
2. Chunhong Zhu, Masayuki Takatera, Effect of Fabric Structure and Yarn on Capillary Liquid Flow within Fabrics, *Journal of Fiber Bioengineering and Informatics*, 6 (2), pp. 205-215, 2013
3. Chunhong Zhu, Masayuki Takatera, A new thermocouple technique for the precise measurement of in-plane capillary water flow within fabrics, *Textile Research Journal*, 84 (5), pp. 513-526, 2014

Acknowledgments

First and foremost, I would like to express my deepest gratitude to my supervisor, Professor Masayuki Takatera, for his valuable guidance, support and encouragement in my academic research work. Special thanks are given to Professor Toyonori Nishimatsu, Professor Masayoshi Kamijo, Professor Shigeru Inui and Professor Morihiro Yoneda for their meticulous comments and advices.

I sincerely appreciate the Grant-in-Aid for Global COE Program awarded by the Ministry of Education, Culture, Sports, Science, and Technology of Japan, the International Fiber Engineering Course of Shinshu University and the Rotary Yoneyama Memorial Foundation for their financial support.

I would like to thank my colleagues in Takatera Laboratory for their generous assistance in every aspect in my life and warm encouragement during my study in Japan.

Finally, I dedicate my greatest thanks to my beloved family, my parents, my brother and Mr Jian Shi. They encourage me to move forward and make my life colorful and meaningful.